OTH 92 379

A CRITERION FOR ASSESSING WIND INDUCED CROSSFLOW VORTEX VIBRATIONS IN WIND SENSITIVE STRUCTURES

Prepared by Brown & Root Limited
for the Health and Safety Executive

Offshore Technology Report

Health and Safety Executive

OTH 92 379

A CRITERION FOR ASSESSING WIND INDUCED CROSSFLOW VORTEX VIBRATIONS IN WIND SENSITIVE STRUCTURES

Author

R W Robinson and J Hamilton

Brown & Root Limited
150 The Broadway
Wimbledon
London SW19 1RX

London: HMSO

Health and Safety Executive - Offshore Technology Report

First published 1992
ISBN 0 11 882032 X

This report is published by the Health and Safety Executive as part of a series of reports of work which has been supported by funds formerly provided by the Department of Energy and lately by the Executive. Neither the Executive, the Department nor the contractors concerned assume any liability for the reports nor do they necessarily reflect the views or policy of the Executive or the Department.

Results, including detailed evaluation and, where relevant, recommendations stemming from their research projects are published in the OTH series of reports.

Background information and data arising from these research projects are published in the OTI series of reports.

TABLE OF CONTENTS

SUMMARY

This document reviews the current state of the art for assessing the sensitivity of offshore structures to wind induced vortex vibrations.

In particular, current methods (DnV, BS8100 and ESDU are discussed) do not offer good guidance on the level of structural damping to be assumed.

Data are presented indicating that the level of structural damping decreases for slender tubulars and appropriate damping values are proposed. Based on these assumptions, a screening method is proposed for tubulars and a methodology presented for assessing the maximum stresses and the fatigue life. This document supersedes the original report OTO 88 021

NOTATION

a	amplitude of vibration
a_s	static deflection under applied load
$a_{\max}$	maximum amplitude of vibration
a_{crit}	maximum amplitude of vibration $V = V_{crit}$
A_i	coefficient for determining natural frequency of a beam, e.g. $2\pi N_s = \frac{Ai}{H^2} \cdot \sqrt{\frac{EI}{M_e}}$ where "i" refers to the type of end fixity
BM	maximum bending moment
$C_{1..}C_6$	ESDU narrow banded force coefficients
Cl_{jb}	broad banded mode average force coefficient
Cl_j	mode averaged lateral force coefficient
D	diameter
E	Young's modulus
F	vortex shedding excitation force per unit length
F_{BM}	bending moment factor $= \frac{BM}{EI \cdot a / H^2}$
H	length or span
I	second moment of interia of the member
I_m	atmospheric turbulence intensity
K_8	damping for foundations
K_e	BS8100 response bandwidth parameter
K_s	stability parameter $= \frac{4\pi \cdot \zeta_s \cdot M_e}{P_a \cdot D^2}$
M_e	effective mass per unit length $M_e =$
M_j	mode averaged mass $= \frac{M_e}{H} \cdot \int_0^H u(z)^2 \, dz$
n	number of load cycles
n_j	natural frequency of mode 'j' in Hz
N	mode shape parameter

N_f	number of cycles to failure
N_v	frequency of vortex shedding in Hz
N_s	natural frequency of vibration of the structure in Hz
$R_{1..}R_5$	ESDU broad banded force coefficients
$u(z)$	mode shape
V	wind velocity normal to member
V_{crit}	velocity for which $N_v = N_s$
V_r	reduced velocity $V_r = \frac{V}{N_s \cdot D}$
R_e	Reynolds number = $\frac{V \cdot D}{v}$
S_f	stiffness (load/unit deflection)
S_G	response parameter $2\pi \cdot St^2 \cdot K_s$
S_t	Strouhal number = $\frac{N_v \cdot D}{V_{crit}}$
t	wall thickness
z	position along member
γ	mode shape parameter (Van der Pol Coefficient)

$$\gamma = \sqrt{\frac{\int_0^H U(Z)^2\,dz}{\int_0^H U(Z)^4\,dz}}$$

ζ_s	structural damping as a fraction of critical
P_a	air density
P_s	steel density
ϵ	surface roughness dimension
Y	ratio of response amplitude to member diameter
η_{rms}	narrow banded rms response amplitude to diameter ratio
η_{Brms}	broad banded rms response amplitude to diameter ratio
σ_r	dynamic stress range
v	kinematic viscosity
δ	logarithmic decrement $=2\pi \cdot \zeta_s$
δ_s	logarithmic decrement taking account of the foundation

ACKNOWLEDGEMENTS

The authors wishes to express their gratitude to Elf Aquitaine Norge A/S and the KEBS Consortium for permission to publish full scale measurements for the Heimdal Platform. They also wish to thank the Engineering Science Data Unit (ESDU) for granting permission to publish extracts from their guidance notes.

In addition the authors would like to thank the members of the UKOOA structural sub-committee, in particular the contributions from BP Exploration, and British Gas, for their comments on this report. Finally the authors would like to express their appreciation.

1. INTRODUCTION

Vortex induced crossflow vibrations of structures in both air and water have been known for some time, and the principal aero/hydro/elastic elements identified.

Reviews of the literature are described in section 2. The principal elements are as follows:

- The vortex shedding frequency N_v is identified by the Strouhal number:

  $$St = \frac{Nv.D}{V_{crit}}$$

  The customary value of St for circular cylinders is St = 0.2 although in practice it depends both on Reynolds number and the amplitude of the resulting vibration.

- If the vortex shedding frequency coincides with a natural frequency of vibration of a member (or an assembly of members), N_s, i.e.:

  $$V = V_{crit} \text{ where } V_{crir} = \frac{D.N_s}{St}$$

  and the damping (structural and fluid) is sufficiently small for the crossflow forces to 'lock on' to the structural natural frequency then large amplitude oscillations result. The velocity is frequently expressed as a reduced velocity defined as:

  $$V_r = \frac{V}{N_s \cdot D}$$

- These large amplitude oscillations self limit when the amplitude of the vibration becomes comparable to the size of the vortex. This limit is found experimentally to be of the order 1 to 1.5 diameters depending on the member mode shape.

- The limit on the amplitude of oscillation is rarely an acceptable limit except for cables, since the resulting strains are too high. For example for a simply supported or encastre beam the maximum strains are given by:

  $$\text{Max strain} = \frac{\pi^2}{2} \cdot \frac{a \cdot D}{H^2} \text{ (simply supported)}$$

  and

  $$= 14.1 \cdot \frac{a \cdot D}{H^2} \text{ (built in)}$$

  For a typical maximum allowable strain of 1/1000, the minimum span/diameter ratios which will not overstrain the member at an amplitude of one diameter are H / D of 70 (simply supported) and 120 (encastre).

- The magnitude of the response is defined by the excitation force and damping. In the latter case the damping is often expressed as a stability parameter or a non-dimensional damping expressed in terms of the structural mass and damping, i.e. K_s. This last term is defined as

  $$K_s = \frac{4\pi \cdot M_e \cdot \zeta_s}{P_a \cdot D^2}$$

As K_s, increases then the response amplitude approximately proportionally decreases when lock-on occurs. Damping in air is almost totally due to structural damping, since aerodynamic fluid damping is negligible.

- In principle for a narrow band excitation, the vibration amplitude can be expressed as:

$$\frac{a}{D} = \frac{Cl}{4\pi \cdot K_s \cdot St^2}$$

Where Cl is a (mode dependent and amplitude dependent) lift coefficient and $2\pi \cdot St^2 \cdot K_s$ is often called the response parameter.

- At wind speeds away from $V = V_{crit}$, the locked-in narrow banded behaviour becomes more episodic, and the response decreases. The range of V / V_{crit} for which the oscillations remain significant is wider for lightly damped structures than for heavily damped structures.

This brief outline points to the dominant role of structural damping in determining the amplitude of wind vortex induced oscillations and the range of excitation wind speeds.

It should be noted that the problem of in-line vortex excitation is not addressed in this document. For guidance on this subject, reference should be made to DEn [20] and Hallam et al [16].

2. CRITIQUE OF CURRENT METHODS

2.1 INTRODUCTION

There are several methods available to the offshore engineer which can be used in assessing the susceptibility of superstructures to wind induced vortex shedding. These include DnV[1], ESDU[2] and BS8100[3]. These are reviewed and compared with laboratory and full scale measurements.

2.2 DnV METHODOLOGY

The DnV method is relatively simple, considering only the effects of mass, wind speed, structural damping and Reynolds number.

2.2.1 Excitation Range

In the case of wind induced crossflow excitation the DnV Rules[1] only identifies the likely range of wind conditions when vortex induced excitation becomes significant. The effect of off-critical response is not considered specifically, except the region of lock-on is limited to $0.94 < V / V_{crit} < 1.6$ as based on a Strouhal number of 0.2. It is assumed that once wind velocities fall within this range then the maximum cross flow response is achieved. No method of accounting for low amplitude broad band cross-flow is presented. The choice of Strouhal number used to assess the critical velocity is defined by the Reynolds number as shown in Figure 2.1.

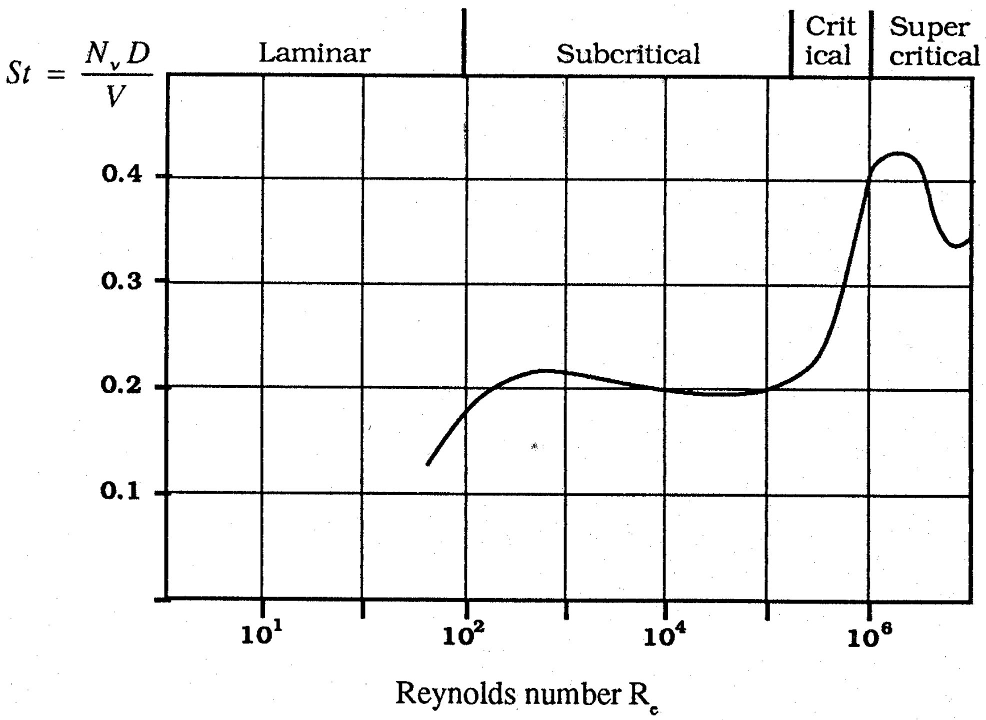

Figure 2.1
DnV, Strouhal number versus
Reynolds number for a circular cylinder

2.2.2 Excitation Forces

Once it has been established that the wind speeds fall within the range for lock-on to occur then the excitation force can be derived. The guidance identifies that the excitation force per unit length is given by:

$$F = \tfrac{1}{2} . \rho_a \cdot Cl \cdot D \cdot V^2$$

where the crossflow force coefficient, *Cl*, is defined by the Reynolds number of the stationary cylinder based on the velocity of the flow past the member as shown in Figure 2.2. Note that the DnV formula above predicts a larger response at the upper limit of lock-on than at V_{crit}

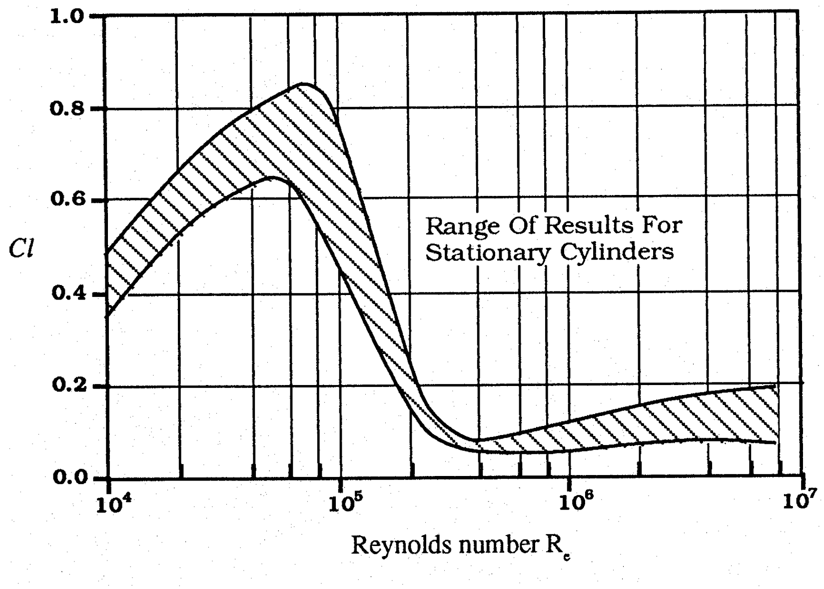

Figure 2.2
DnV, fluctuating crossflow force coefficient
versus Reynolds number for a smooth circular cylinder

2.2.3 Response Amplitude

The response amplitude can then be derived at lock-on from the force over damping ratio for the member, i.e:

$$a = \frac{a_s}{2\zeta_s}$$

Where typically

$$a_s = \frac{F}{S_f}$$

is the 'static' deflection with S_f the stiffness {load IFI to give unit deflection}, and where ζ_s is the structural damping expressed as a fraction of critical damping. DnV recommend that the structural damping contribution used in calculating the response is 0.5% critical. It is worth noting that the DnV Rules makes use, for current flows, of a threshold value of the stability parameter, K_s of 16 above which the response amplitudes can be considered non-consequential. However for vortex induced excitation in air it does not recommend a threshold value for the stability parameter.

2.3 ESDU METHODOLOGY

The ESDU methodology [2] is considerably more detailed than the DnV method taking into account many more parametric effects. No attempt is made here to give a description of the detailed procedure outlined in ESDU Note 85038, but rather the simplified more conservative method contained in ESDU Note 85039 is presented and the parametric effects identified. These consist of:

- Roughness of the vortex generation surface
- The effect of atmospheric turbulence
- Spanwise correlation due to end effects
- Effect of mode shape on the excitation force
- Influence of the response amplitude on the excitation force
- Reduction of response as the wind velocity deviates from the critical wind velocity
- Effects of tapered or stepped diameter members
- Prediction of low amplitude broad banded responses

The basic technique is to derive the response amplitude at the critical velocity as a function of damping using the standard equations for the member properties. The response is then calculated by interpolating the derived function for the correct value of structural damping.

In the case of non-critical wind velocities the response can be corrected based on the damping level and response amplitude at the critical velocity and for low amplitude broad banded responses a modified set of equations are presented and used.

2.3.1 Excitation Range

The range in which significant levels of response can be achieved is defined by the stability parameter K_s as shown in Figure 2.3. For values of K_s less than 24 ($M\zeta_s / P_a D^2 = 1.9$), the response amplitude exceeds more than 10% of the member diameter for V/V_{crit} of 0.85, the guidance notes suggest that the responses drop rapidly for V/V_{crit} less than this value and that it corresponds to the onset velocity for lock-on. Similar effects were noted for V/V_{crit} greater than 1.5 although the guidance recommends that buffeting should be considered as an excitation mechanism for values exceeding 1.2.

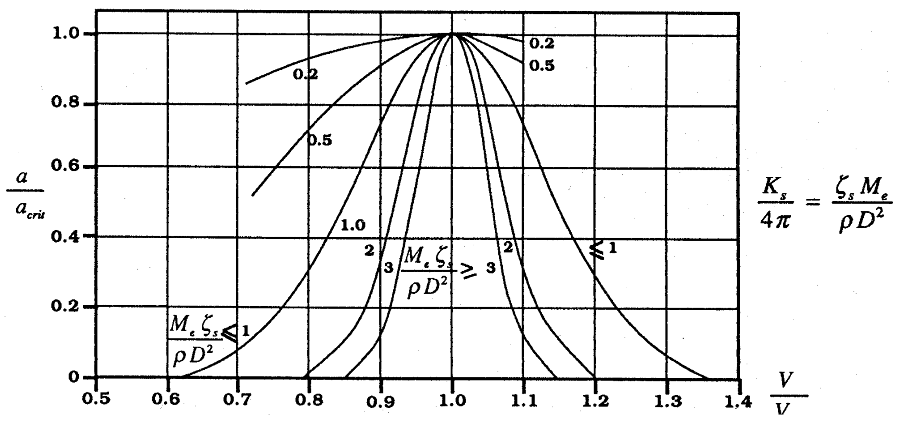

Figure 2.3
ESDU 85039, narrow banded response envelope curves

In the case of broad banded responses the full response envelope defined by the stability parameter should be used based on the turbulence coefficient as shown in Figure 2.4 (for further definition see [2].

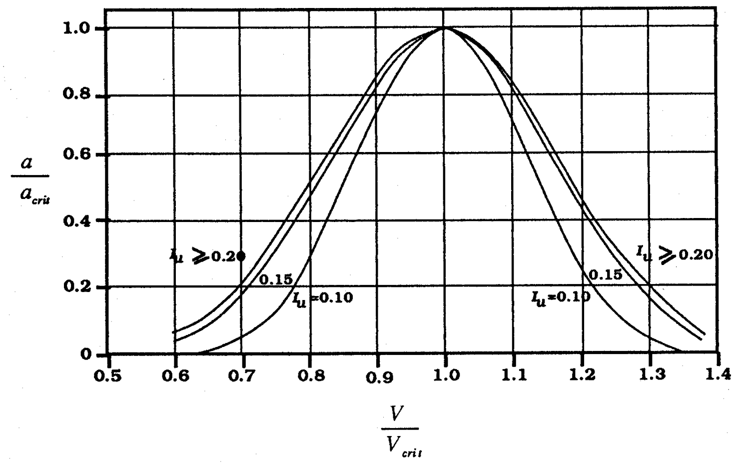

Figure 2.4
ESDU 85039, broad banded response envelope curves

When calculating the critical velocity in either case the Strouhal number should be determined based on the Reynolds number and the response amplitude as shown in Figure 2.5.

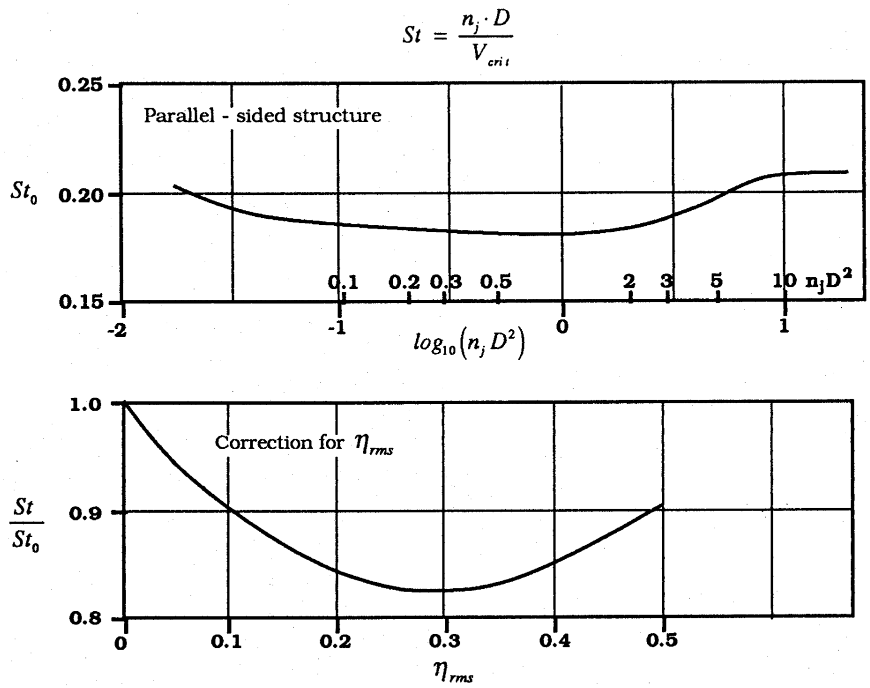

Figure 2.5
ESDU 85039, Strouhal number for critical flow velocity and response

2.3.2 Excitation Force

The excitation force per unit length when the wind speed corresponds to the critical velocity is given by:

$$F = \tfrac{1}{2}.p_a.Cl_j.D.V^2_{crit}$$

where Cl_j is the mode averaged lateral force coefficient and is derived from a number of component coefficients for narrow banded responses defined as:

$$Cl_j = C_1.C_2.C_3.C_4.C_5.C_6.St^2$$

where the coefficients are defined in Figure 2.6 and have the following significance:

C_1 Coefficient defining the variation of the lift coefficient for the stationary cylinder as a function of the Reynolds number at the critical velocity, ie N_sD^2/vSt

C_2 Coefficient defining the effects of cylinder roughness on the excitation force where roughness is defined as ε /D

C_3 Coefficient defining the effect of mode shape on the excitation force as defined by the mode shape parameter N

C_4 Coefficient defining the influence of end effects and spanwise coherences on the excitation force as defined by the length to diameter ration H/D depending on the Reynolds number at the critical velocity

C_5 Coefficient defining the effect of the flow turbulence intensity I_u on the excitation force

C_6 Modification coefficient to correct the lift coefficient for flow past a stationary cylinder when that member is moving at a given amplitude signifying the degree of lock-on

N.B. $M_j = \frac{1}{2}M_e$ for pinned/pinned uniform beam first mode vibration, and $a_{max} = \sqrt{2}.D.\eta_{rms}$ for narrow banded response and 0.00633 = $1/16\pi^2$. The term St^2 is introduced to preserve the normal formulae for η_{rms} below, but in practice is cancelled out.

The coefficients C_1 .. C_6 follow the recommendations of the more detailed methodology described in ESDU Note 85038 except for the coefficient C_4. In ESDU Note 85038, increasing *H/D* causes the spanwise coherence to drop considerably more rapidly than shown by the coefficient C_4 in figure 2.6.

In the case where the response amplitude does not exceed 2% of the member diameter than the response can be treated as broad banded rather than narrow banded. In this case the excitation force per unit length when the wind speed corresponds to the critical velocity is given by:

$$F = \tfrac{1}{2}.p_a.D.Cl_{jb}.V^2_{crit}$$

where Cl_{jb} is the mode averaged lateral force coefficient and is derived from a number of component coefficients for broad banded responses defined as:

$$Cl_{jb} = R_1.R_2.R_3.R_4.R_5.St^2$$

where the coefficients are defined in Figure 2.7. Note that the coefficients R_1 to R_5 have the same significance as C_1 to C_5 but have slightly different values in some cases. In the case of broad banded response there is no enhancement of the excitation force due to lock-on.

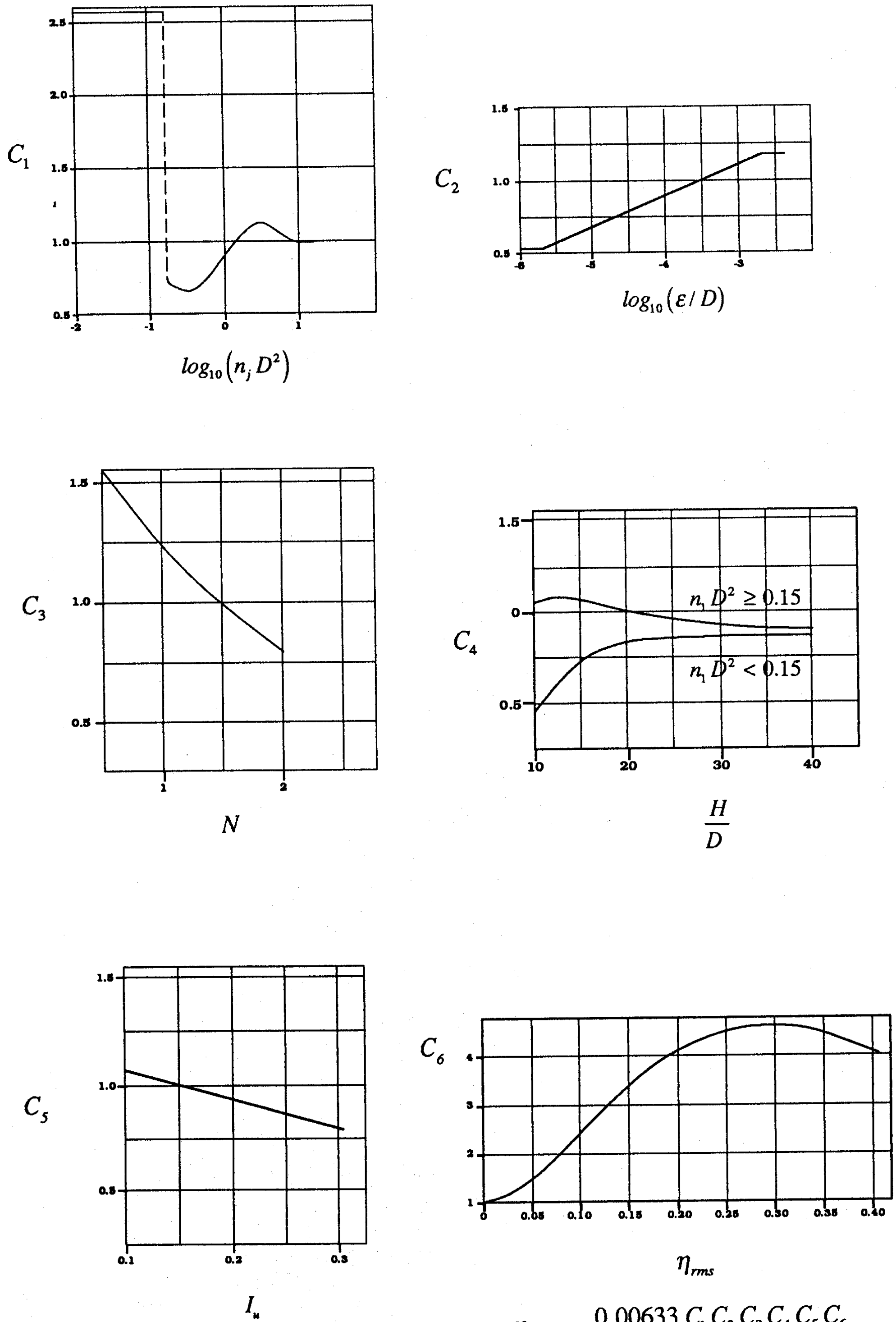

$$\eta_{rms} = \frac{0.00633\, C_1 C_2 C_3 C_4 C_5 C_6}{M_e \zeta_s / \rho D^2}$$

Figure 2.6
ESDU 85039, excitation force coefficients for narrow banded, lock-on responses

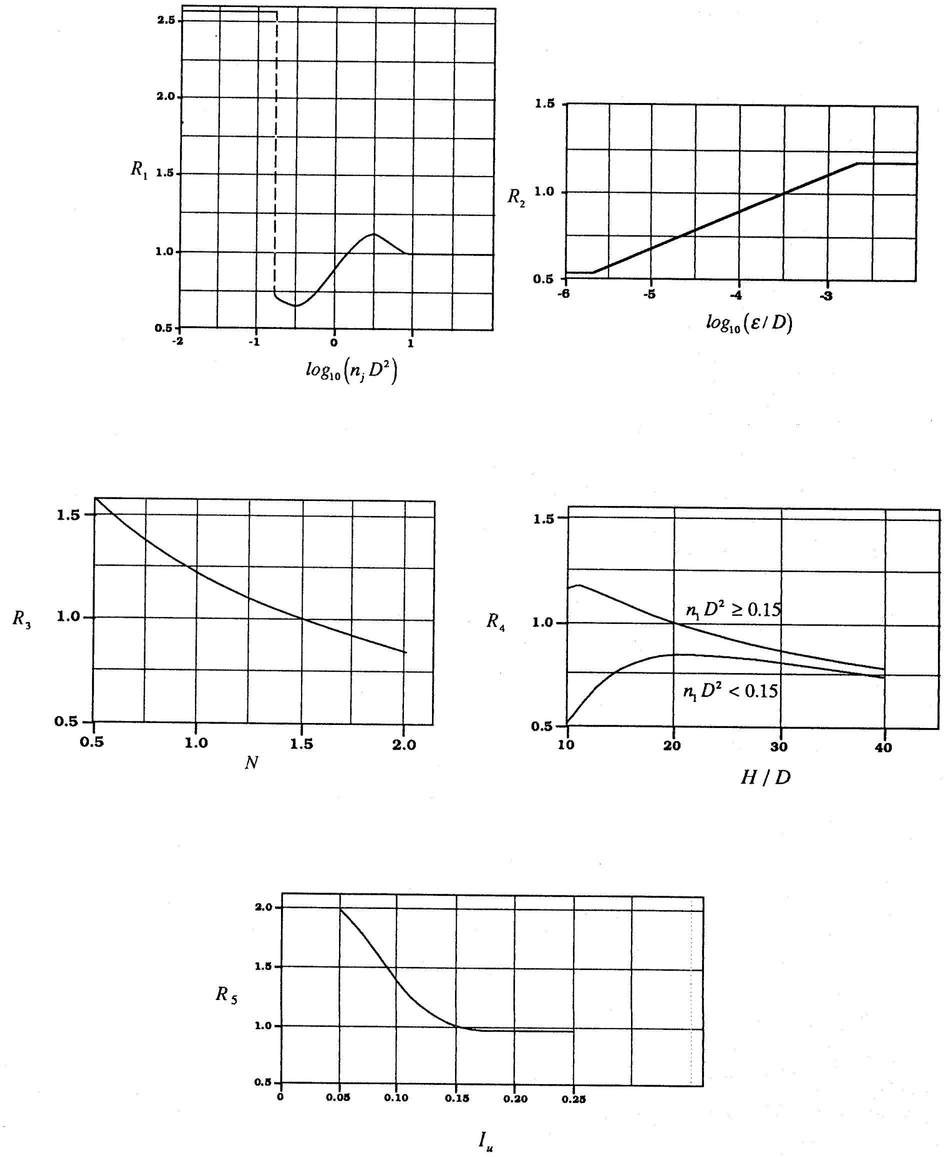

$$\eta_{Brms} = \frac{0.0162\ R_1 R_2 R_3 R_4 R_5}{M_j\ \zeta_s^{1/2} / \rho D^2}$$

Figure 2.7
ESDU 85039, excitation force coefficients
for broad banded responses

2.3.3 Response Amplitude

In the case of narrow banded responses at the critical velocity the response amplitude is defined by:

$$\eta_{rms} = \frac{Cl_j}{4\pi K_s St^2} \cdot \frac{M_j}{M_e}$$

or

$$\frac{Cl_j}{16\pi^2 St^2 M_j(\zeta_s/\rho_a D^2)}$$

and

$$\frac{a}{D} = \sqrt{2}\,.\eta_{rms}$$

In the case of broad banded response (ieη_{rms} < 0.02) at the critical velocity the response amplitude is given by:

$$\eta_{Brms} = 2.56\sqrt{\zeta_s} \cdot \frac{Cl_{jb}}{4\pi K_s St^2(M_j/M_e)}$$

$$= 2.56\ \sqrt{\zeta_s} \cdot \frac{Cl_{jb}}{16\pi^2 \zeta_s St^2(M_j/\rho_a D^2)}$$

and

$$\frac{a}{D} = 4\eta_{Brms}$$

Note: M_j/M_e is similar to the inverse of the Van der Pol coefficient, ie.

$$\frac{M_j}{M_e} = \frac{1}{H} \cdot \int_O^H u(z)^2 dz$$

and

$$\gamma = \sqrt{\frac{\int_O^H u(z)^2 dz}{\int_O^H u(z)^4 dz}}$$

For velocities other than the critical velocity the maximum response is reduced as based on the response envelopes discussed in Section 2.3.1.

When evaluating the stability parameter *Ks*, ESDU recommend various levels for structural damping as shown in Table 2.1. In the case of steel cantilever structures such as flarebooms which are supported on a steel substructure the level of damping recommended lies between 0.3% and 0.5%. However for steel tubes a higher level of damping of between 0.5% and 1% is recommended.

Table 2.1
ESDU 85038, recommended structural damping levels

Structure	ζ_s(%) Minimum	Maximum
Steel stack or tower, unlined, welded, firm foundation	0.4	0.6
Steel stack or tower, unlined, welded, soft soil	0.5	0.7
Steel stack or tower, unlined, bolted, firm foundation	0.6	0.9
Steel stack or tower, unlined, bolted, soft soil	0.7	1.0
Steel stack or tower, unlined, welded, elevated on steel support structure		
	0.3	0.5
With lining (at least 50mm thick) add 0.002 to the above values		
Concrete stack or tower		
Concrete stack with internal flues	0.5	1.2
	1.2	2.5
Aluminium (aluminium) alloy tubes		
	0.08	0.2
Steel tubes		
	0.5	1.0

2.4 BS8100 METHODOLOGY

The BS8100 Code of Practice for the design of Lattice Towers and Masts, Part 1 Code of Practice for Loading, is a new BS code released in 1986 which provides design guidance on cross-wind response due to vortex shedding. The procedure is a simplified procedure similar to the DnV method with the following features.

2.4.1 Excitation Ranges

The critical wind speed at which structures are subjected to cross-wind excitation is given by the same relationship that adopted by DnV and ESDU. However the Strouhal number is fixed as 0.2 for circular cylinders and 0.15 for sharp edged structural elements. The code makes no reference to broad banded resonance response. In the case of narrow banded lock-on the velocity above which lock-on is predicted is identified as V=0.77 V_{crit} and the response envelope for both circular and bluff cylinders is as shown in Figure 2.8. The upper bound limit for a circular cylinder is identified as V = 1.38 V_{crit}.

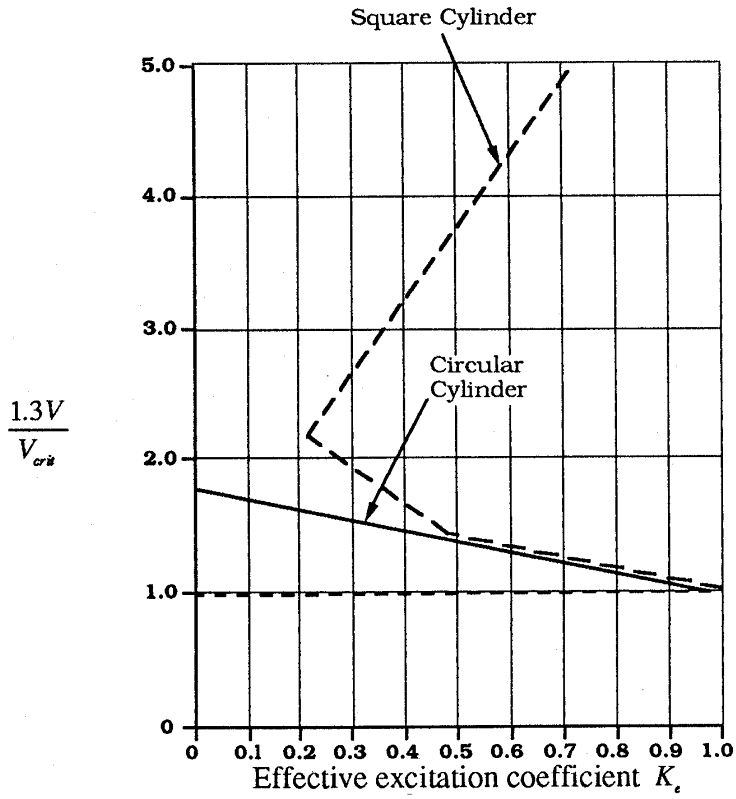

Figure 2.8
BS 8100, response envelope curves

2.4.2 Excitation Forces

Once the threshold velocity is exceeded the code recommends that the amplitude of vibration should be derived. The excitation force per unit length acting on the member is given by the relationship:

$$F = 0.9\rho_a.V^2.K_e.Cl.D.\sin(2\pi N_s t)$$

The aerodynamic lateral coefficient Cl is given as 0.3 for circular cylinders and 0.5 for bluff bodies and K_e is the response envelope parameter which allows a reduction in response when the wind velocity deviates from the critical velocity.

2.4.3 Response Amplitudes

The code does not provide direct guidance on deriving the response amplitude but recommends that the response be derived from dynamic analysis using the equation for the excitation force shown above. However it does recommend structural and aerodynamic damping for the structure to be used in the dynamic analysis as shown in Table 2.2. These damping levels can be enhanced when the structure is mounted on a flexible foundation. In the case of welded steel bracing the code recommends a structural damping level of 0.24%.

Table 2.2
BS 8100, recommended structural damping levels

Table E.1 Logarithmic decrements of damping δ_T for tower superstructure

Nature of structural connections	Surface finish at connections	Logarithmic decrement δ_T	ζ_s(%)
All welded or all friction grip or fitted bolted	All finishes	0.01	0.24
Welded bracings: bolted flange plate connection to legs	All finishes	0.015	0.24
Welded bracings: black bolted gusset connection to legs	Clean, unpainted:	0.06	0.95
	Gritblasted, metalsprayed:	0.045	0.72
	Galvanized:	0.03	0.48
Black bolted bracing: bolted flange plate connection to legs	Clean, unpainted:	0.04	0.64
	Gritblasted, metalsprayed:	0.03	0.48
	Galvanized:	0.02	0.32
Black bolted bracing: black bolted gusset connection to legs	Clean, unpainted:	0.08	1.27
	Gritblasted, metalsprayed:	0.06	0.95
	Galvanized:	0.04	0.64

Table E.2 Damping factor, K_δ, for various types of foundation

Type of foundation	Factor
Piled foundation or spread footing stiff soil or rock	1
Spread footing on medium stiff soil	1.5
Spread footing on soft soil	3

$$\delta_s = K_s \delta_T$$

δ_s= logarithmic decrement including soil effects

2.5 EMPIRICAL DATA

The parametric influences and coefficients identified in each of the analysis procedures have been compared to the experimental evidence presented in the literature especially where there was a conflict in the recommendation of certain parameters. It should be noted that the literature search was not exhaustive.

2.5.1 Excitation Ranges

Each of the methods proposed identified different threshold values for wind velocity as based on the reduced velocity or the ration of velocity to critical velocity. Figure 2.9 shows a comparison of threshold velocities at which synchronised vortex shedding (lock-on) was observed as a function of response amplitude for four data sets as determined by Woo et al [4], Peltzer [5], Standsby[6] and Koopman[7]. These results show that the threshold boundaries increase with response amplitude (*a/D*) up to ratios of 0.3 but limit at $0.8<V/V_{crit}<1.5$ for amplitudes exceeding this value. However there is evidence from the work of Patrikalakis and Chryssostomidis[8] that the upper limit may extend to as high as 2.25 for large amplitude oscillations in a uniform stream and Standsby[6] identified significant oscillations for V/V_{crit} as low as 0.7.

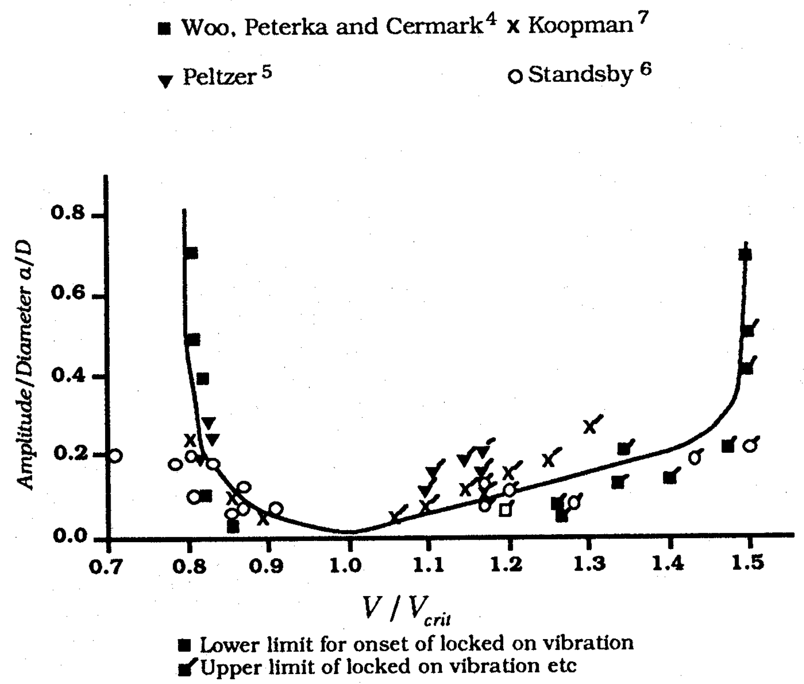

Figure 2.9
Lock-on response boundaries versus response amplitude

Whereas DnV does not allow for any fall-off in response as the velocity deviates from the critical value, the ESDU and BS 8100 methods do allow for such. The comparison of the response envelope as predicted by ESDU is shown in Figure 2.10 compared with measured response levels from the results of Feng[9] and Patrikalakis and Chryssotomidis[8]. These comparisons reveal that the bandwith response predicted by ESDU could be valid for low amplitude oscillations, but underestimates the lock-on ranges at large amplitudes.

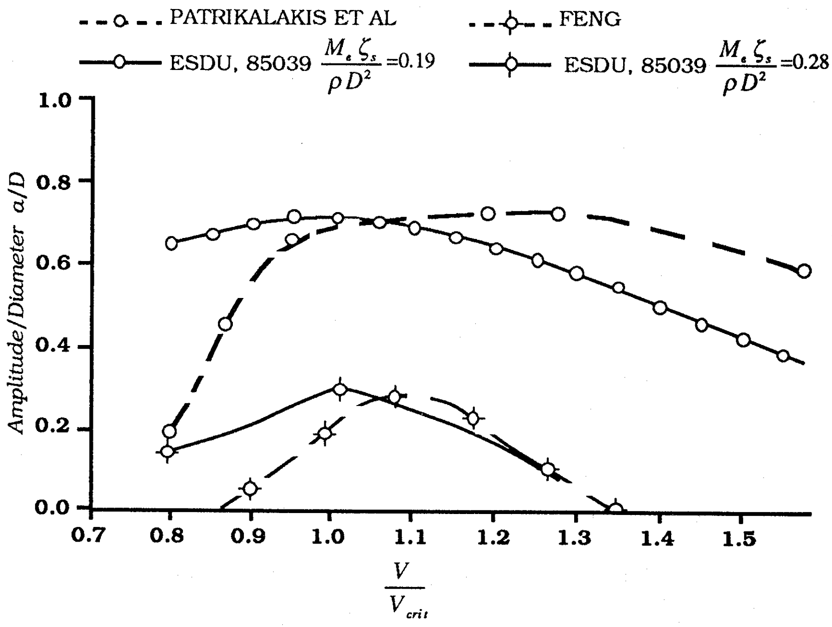

Figure 2.10
Response envelope for increasing amplitude

2.5.2 Excitation Forces

The variation of the static lift coefficient with Reynolds number is well supported in the experimental evidence as contained in Sarpkaya and Isaacson[10], see Figure 2.11. However the experimental data show a high degree of scatter which may be attributed to some of the other parametric effects identified by ESDU such as surface roughness or lift enhancement when the member is vibrating. The DnV range of lift coefficients is shown superimposed on the experimental data in Figure 2.11.

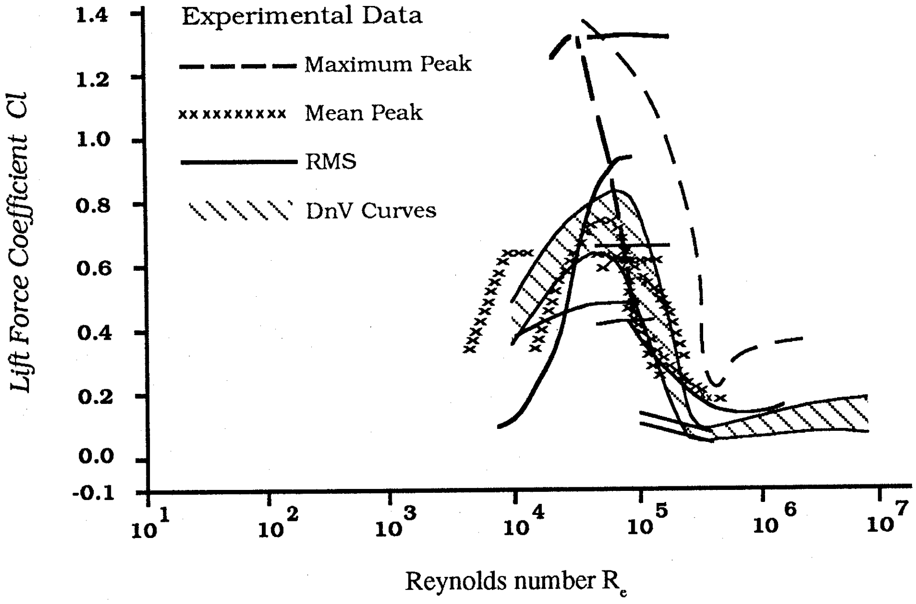

Figure 2.11
Experimental lift force coefficients versus Reynolds number

The influence of response on the lift coefficient proposed by ESDU is supported by the results of Vickery and Watkins[11] and Hartlen et al[12] published in Blevins[13] and shown in Figure 2.12. These results indicate that there is an enhancement in the lift coefficient as the vibration amplitude increases to about 0.3 diameters but beyond that the excitation force reduced and eventually disappears as the amplitude approach the self limiting value of about 1.5 diameters.

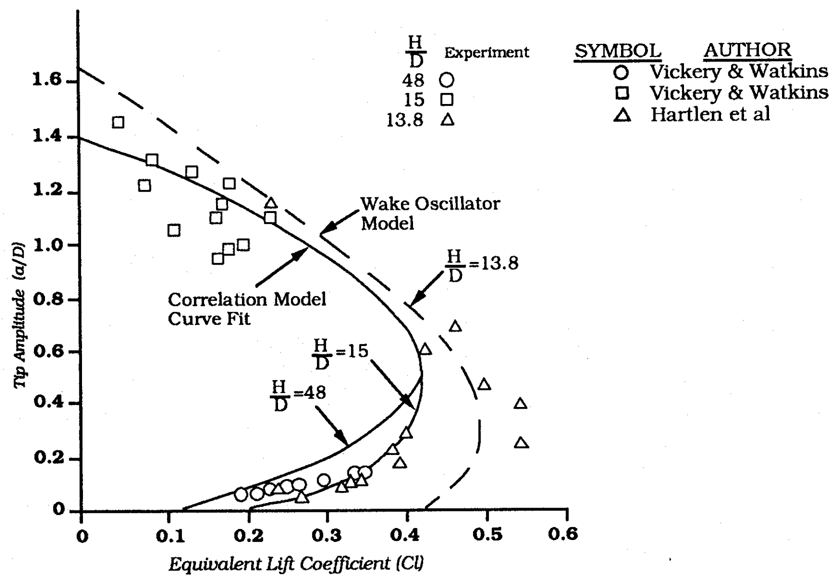

Figure 2.12
Influence of response on excitation force

The influence of end effects and coherent length as a function of the diameter to span ratio are shown in Figure 2.13 (published by Blevins[13] as based on the work of Toebes[14]). It should be noted that the coherent length increases as the amplitude over diameter ration of the cylinder increases. The same effect has been noted by Vandiver[15] as shown in Figure 2.14.

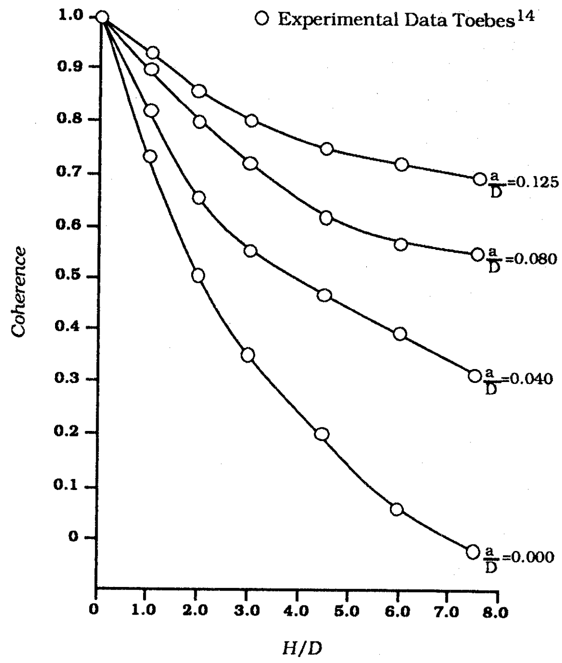

Figure 2.13
Spanswise coherence versus span/diameter ration (Toebes[14])

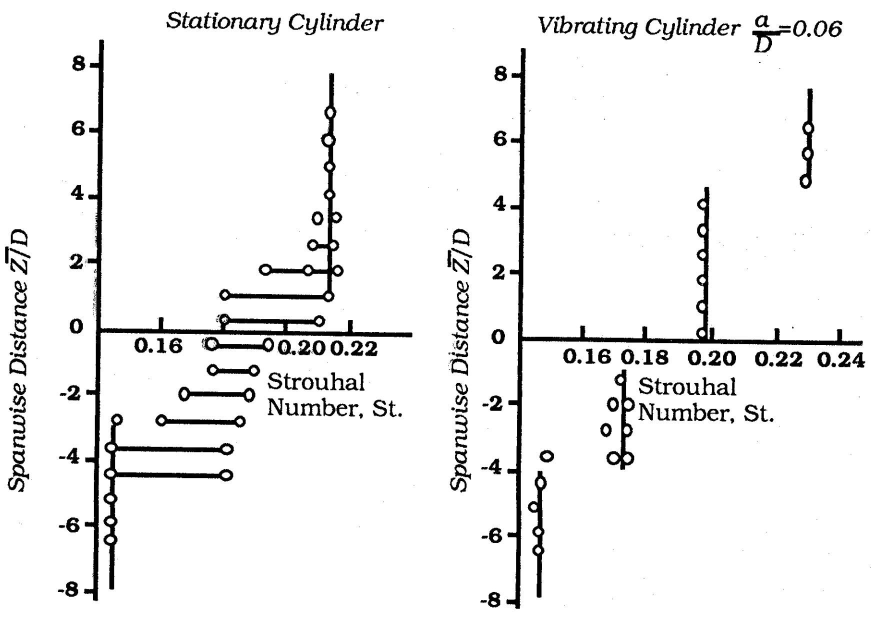

Figure 2.14
Coherent lengths of stationary and
vibrating cylinders in a sheared flow (Standsby[6])

who noted from the results published by Standsby[6] that the variation of Strouhal number along the length of a vibrating member behaved in a more cellular manner than that of the corresponding stationary cylinder indicating increased coherence as the vibration amplitude increases.

These results would indicate that the effects of loss of spanwise coherences for an oscillating member are self-limiting ie there is an initial loss of coherence with increasing span to diameter ratio but the reduction in the excitation force due to loss of coherence reaches an asymptotic value when the span to diameter ration exceeds about 10. At significant levels of response, ie a non-stationary cylinder, this data does not support the effect documented in the detailed ESDU Note 85038 but is more consistent with the simplified methodology in ESDU Note 85039.

Blevins[13] and Sarpkaya and Issacson[10] have demonstrated that the influence of the member mode shape influences the maximum response amplitude of a vibrating cylinder. Table 2.3 shows the variation of the limiting response amplitude with the mode shape parameter N defined as:

$$N = \frac{1}{2}\cdot\left(\frac{H}{\int_O^H u(z)^2 dz} - 1\right)$$

and the Van der Pol coefficient

$$\gamma = \sqrt{\frac{\int_O^H u(z)^2 dz}{\int_O^H u(z)^4 dz}}$$

where u(z) is the mode shape. Example values for *N* are given below:

N=	0.5	Pin-ended member	
	1.5 - 2.0	Cantilever	: first mode
	3.0 - 5.0	Cantilever	: second mode
	0.76	Clamped	: first mode
	0.64	Clamped	: pinned first mode

Table 2.3
Influence of mode shape parameter on maximum response amplitude

Mode type	Mode shape parameter N	Van der Pol coefficient γ	Maximum Amplitude/diameter Blevins[13]	Sarpkaya[10]	ESDU*[2]
u(z)=z/H Pivoted cantilever	1	1.305	1.40	1.68	1.45
u(z)=sin(πz/H) Pin-ended beam	0.5	1.155	1.20	1.50	1.25
u(z) = 1.0 Rigid beam	0.0	1.00	1.00	1.30	1.00

- Corrected for $\int_O^H u(z)^2\, dz$ effect and normalised at N=0

In general the higher the mode shape parameter N then the greater is the limiting vibration amplitude. Subsequently the vibration mode shape should be taken into account when predicting the response of a structural member. The results from Sarpkaya and Issacson[10] are about 30% higher than those from Blevins[13]. This variation is due to the conservative assumptions inherent in the wake oscillator models as described in Sarpkaya as against the empirical data described in Blevins.

2.5.3 Response Amplitudes

Blevins[13] demonstrates the significance of the structural damping estimate in terms of defining member response as shown in Figure 2.15 for rigid cylinder (N=0). Clearly for typical levels of damping ($2\pi K_s St^2$) the variation of response is inversely proportional to damping and a 50% error in the estimate of damping will lead to 50% error predicting the response.

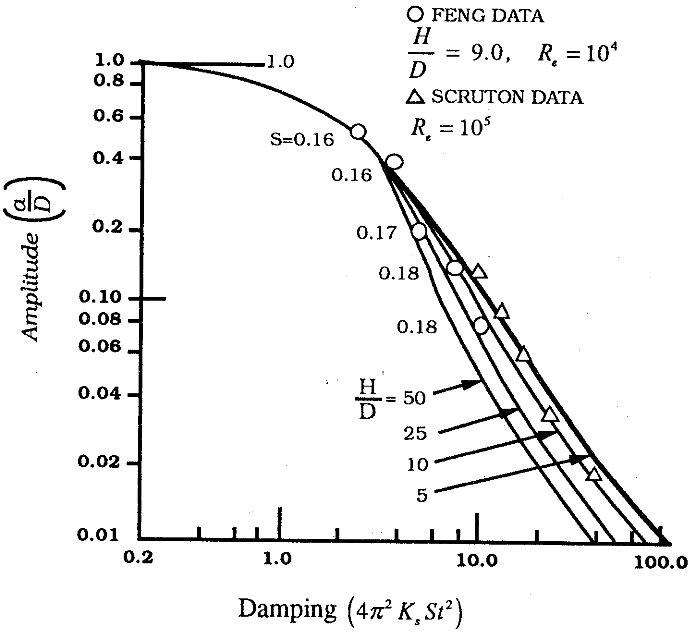

Figure 2.15
Response versus stability parameter for a rigid vibrating cylinder
Based on Blevins[13] wake oscillator model

There is very little information in the literature as to the recommended level of structural damping for structural members and component elements of welded steel structures and much of this is wide ranging. Most of the information published is data measured for tower or lattice structures where the damping contribution from the foundations may be considerable but is not relevant to vibrations developing within a sub-structure or a member within a steel Lattice structure.

For example Blevins[13] quotes the variation of structural damping for welded unlined tower structures to vary between 0.16% and 1% with an average value of 0.5% critical damping. The scatter in damping values may be more to do with the damping contributions from the tower foundations than with scatter in the experimental measurement. Hallam et al[16] recommends that a value of 0.32% critical damping be used for fabricated steel but that structural damping for spring steel (unfabricated) could be as low as 0.06% to 0.12%. Overall damping levels for integral steel structures without foundation contributions, as quoted by Hallam et al[16] recommend that a value of 0.32% critical damping be used for fabricated steel but that structural damping fro spring steel (unfabricated) could be as low as 0.06% to 0.12%. Overall damping levels for integral steel structures without foundation contributions, as quoted by Hallam et al[16] lie between 0.16% and 1.3.

These data sources indicate that structural damping is influenced by three factors, ie:

i) The contributions to damping from foundation and soil effects. If the vibrating structure does not produce sizeable vibrations at the foundations then care should be taken that the estimate of structural damping used does not include such.

ii) The effects of fabrication. The manner of construction influences the structural damping eg bolted as against welded structures. Also the effect of fabricating a structure of component steel tubes may lead to higher damping as the nodes become a source of damping due to heat generation as the structure flexes. However for individual members the damping contributions from the joints become increasingly insignificant as the member span to diameter ratio increases.

iii) The type of material out of which the member is manufactured, eg steel, aluminium or steel/concrete composite.

In view of these observations and the importance damping plays in predicting vortex induced oscillations it is advisable that any method should attempt to address these effects and allow for a more exact prediction of structural damping.

Figure 2.15 also demonstrates that, as discussed in Section 2.5.2, the effect of increasing span to diameter ratios could lead to a reduced response. For example, given the same damping characteristics for a *H/D* ratio of 50, the response amplitude is 10% of the member diameter, whereas for a *H/D* ratio of 10 the vibration amplitude is twice as large, ie 20% of the member diameter. However for response amplitudes exceeding 0.4 diameters the sensitivity to span to diameter ratios disappears.

2.6 FULL SCALE OBSERVATIONS

During August 1984 an approximately 120 metre long inclined flare boom was installed on the Heimdal oil production platform in the Norwegian sector of the North Sea. This boom had been designed using the DnV methodology outlined above, with the 0.5% critical damping value quoted. A limiting value of K_s equal to 16 had been agreed with DnV as the limiting design stability parameter.

Observations of vibrations were made in certain wind conditions shortly after its construction and investigations were implemented by the operator consisting of daily observation reports, a program of natural frequency and damping measurements of vibrating members, and inspection of nodes and remedial works reported by Doucet and Nordhus[17]. The vibrations were attributed to vortex induced vibrations in some of the individual truss members and frames. By January 1985 fatigue cracks were found in two of the members. The problems were subsequently resolved by the use of shrouds and tensioned cables attached to the critical members.

During the investigative phase the information acquired has provided some valuable insight into the behaviour of offshore flare structures as discussed in the following sections.

2.6.1 Excitation Ranges

The daily three hour reports taken during the investigative phase identified the wind speed and direction and an estimate of the response amplitude and frequency of those members visibly vibrating, ie ranges of 10mm or greater. The wind speed reports for one member on the upper face were examined in detail and the resolved component of wind speed normal to the member determined as based on the wind speed and direction as shown in Table 2.4. This data gives some evidence of the velocity ranges associated with significant vibrations, ie greater than 4% but tends to be limited to the higher wind speeds. An examination of the ration of the resolved velocity with respect to the critical velocity identified that visible amplitudes of vibration of between 5 and 20% of the member diameter were observed when the *V/Vcrit* lay between 0.83 and 1.45 as based on an assumed natural period as shown in Table 2.4. The critical velocity was based on an assessment of the natural frequency of the member based on using a simple beam analysis, a sub-frame analysis and observed vibration frequencies. The accuracy of the data was insufficient to allow an assessment of either definitive boundary limits or responses within these limits.

Table 2.4
Heimdal flare boom excitation velocities and Reynolds numbers

Windspeed (m/s)	Direction (degs)	Vibration amplitude (mm)	Resolved velocity (m/s)	Reynolds number	V/V_{crit} (N_s=5.2)	V/V_{crit} (N_s=3.8)	V/V_{crit} (N_s=6.8)
22.0	145	10	8.98	$1.88\text{x}50^5$	1.27	1.76	0.97
22.0	150	Small	7.16	$1.50\text{x}10^5$	1.01	1.37	0.77
30.0	20	Small	10.43	$2.16\text{x}10^5$	1.45	1.98	1.11
18.0	150	30-40	5.86	$1.23\text{x}10^5$	0.83	1.14	0.65

		Analysis Type	Natural frequency(Hz)
assumed Strouhal number	0.2		
Member diameter (mm)	273	Simply supported	3.22
Wall thickness (mm)	7.8	encastre	7.18
Length (m)	15.2	Sub-frame analysis frame action	3.80
Kinematic viscosity (m^2/s)	1.3×10^{-5}	Sub-frame analysis member action	6.80
		observed	3.0-4.0
		assumed	5.2

2.6.2 Excitation Force

While it was not possible to measure the excitation forces acting on the members it was noted that as shown in Table 2.4, the associated Reynolds numbers remained sub-critical ie in the range of 1.2 to 2.2 x 10^5.

2.6.3 Response Amplitudes

The design approach using a limit stability parameter of K_s, equal to 16 had been selected to prevent lock-on occurring and maintain vibration amplitudes of less than 4%. However, the observed vibration levels, as shown in Table 2.4, were as high as 15%. Experimental results had supported the premise that a K_s of 16 should prevent amplitudes exceeding 2% as shown in Figure 2.15 and the reason that the vibrations occurred was thought to lie in the choice of parameters used to define the stability parameter and in particular the structural damping.

During the course of the investigation full scale measurements were taken of the structural damping of members which were found to be vibrating, and the results determined as shown in Table 2.5.

Table 2.5
Heimdal flareboom natural frequency and damping data

Member ID	Diameter (m)	Span/Dia H/D	Damping (%crit)	Natural Frequencies (Hz) Measured	Simply supported	Encastre
293-318	0.1683	30.9	0.80	7.8	17.4	39.6
			1.10	2.25		
230-234	0.2191	43.4	1.20	8.5	6.5	14.8
			1.10	26.2		
273-274	0.2191	43.4	0.30	12.1	6.5	14.8
			0.36	13.8		
313-314	0.2730	46.9	0/60	10.5	4.7	10.6
			0.90	24.5		
230-212	0.17	47.5	0.20	15.2	7.4	16.7
			0.30	15.8		

This table shows there is a wide spread of measured natural frequencies for apparently similar members. However there was some possible corruption of the data due to the presence of scaffolding on adjacent trusses. These observations however demonstrate the possibility of structural damping rates as low as 0.2% critical for these high aspect ration trusses, ie *H/D* of about 40-50.

Note that assuming a damping value of 0.2% instead of 0.5% as used in the original analysis, the conventional limit design value of K_s greater than 16, would have prevented the observed vibrations in all but one of the members of the Heimdal flare boom.

2.7 COMPARISON OF METHODS AND DEVELOPMENT OF A SIMPLIFIED PROCEDURE

The DnV method of assessing wind induced vortex shedding responses had been compared to the ESDU, BS8100 and the empirical information consisting of model scale and full scale measurements. The purpose of this comparison was to develop a more accurate simplified procedure which was more consistent with other guidelines and measured data. The review was performed based on discussion of the definition of excitation range and the quantification of the excitation force and response.

2.7.1 Excitation Range

The onset of “locked-on” vortex shedding excitation was found to lie between the *V/Vcrit* range of 0.8 to 1.5 when vibration amplitudes exceed 20% based on empirical measurements as shown in Figure 2.16. This was consistent with the wind velocities in which vortex induced vibrations were observed on the Heimdal flareboom as shown in Table 2.4. However there is some evidence that the lower threshold onset may be as low as 0.7 and the upper threshold as high as 2.0.

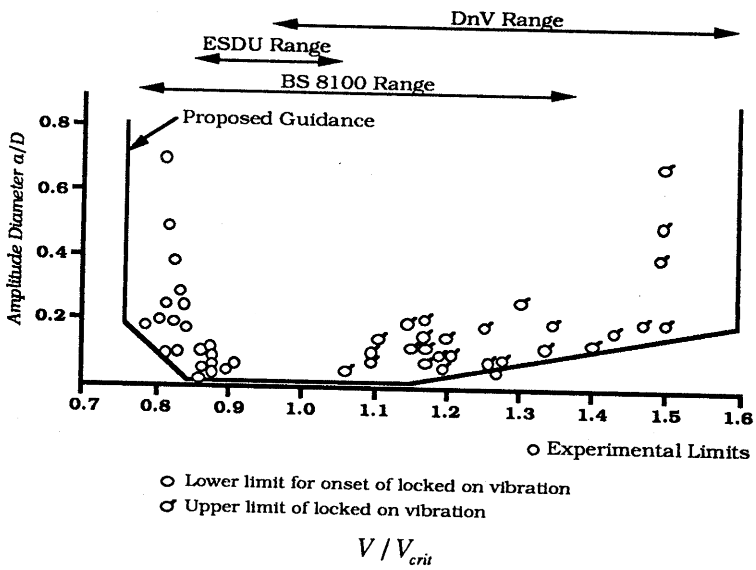

Figure 2.16
Comparison of lock-on boundaries
From DnV, ESDU and BS 8100

The measured data threshold of between 0.7 and 0.8 for amplitudes exceeding 20% of the member diameter compares favourably with the BS8100 recommendation of 0.75. However it is lower than the ESDU lower limit recommendation of 0.85 and the DnV limit 0.94. In both these codes, the experimental evidence indicates that should the amplitude of oscillation exceed 20% of the member diameter at the critical velocity as based on the member damping characteristics and excitation force, then these codes could be non-conservative. In essence, the ESDU lower limit is only valid for response amplitudes of less than 8% and the DnV criteria for amplitudes of less than 2.5%.

It is recommended that the lower limit should be based on the BS8100 threshold value of 0.75. However, if the amplitude of oscillation can be demonstrated to be less than 20%, the lower limit threshold could be increased in accordance with Figure 2.16.

In the case of upper bounds limits, the experimental evidence indicates that the velocity ratio can increase to 1.5 for vibration amplitudes exceeding 20% of the member diameter. This limit compares well wit the DnV criteria of 1.6 but is higher than the ESDU limit of 1.05 and the BS8100 limit of 1.38. It is recommended that for amplitudes of vibration exceeding 20% of the member diameter that the DnV limit of 1.6 should be adopted provided a higher mode is not excited. If the latter occurs, then the critical velocity for the mode closest to the wind velocity should be used to identify which response mode dominates.

Where the vibration amplitude is less than 20% of the member diameter, as based on the critical velocity, the upper bound limit could be reduced in accordance with the response amplitude as shown in Figure 2.16.

Where the vibration is less than 2%, then it can be considered that the response is broad banded and the response determined in accordance with the ESDU guidelines.

Since the response is dictated by the damping of the member, as shown in Figure 2.17, then the lock-on boundary limit can be redefined in terms of the stability parameter rather than the response as shown in Figure 2.18. The stability parameter is defined by the geometric properties of the member so that the lock-on boundaries for a particular member can be quickly assessed. When the stability parameter exceeds 20, then the response falls beneath the critical amplitude of 2% of the member diameter and broad band random response results rather than narrow .

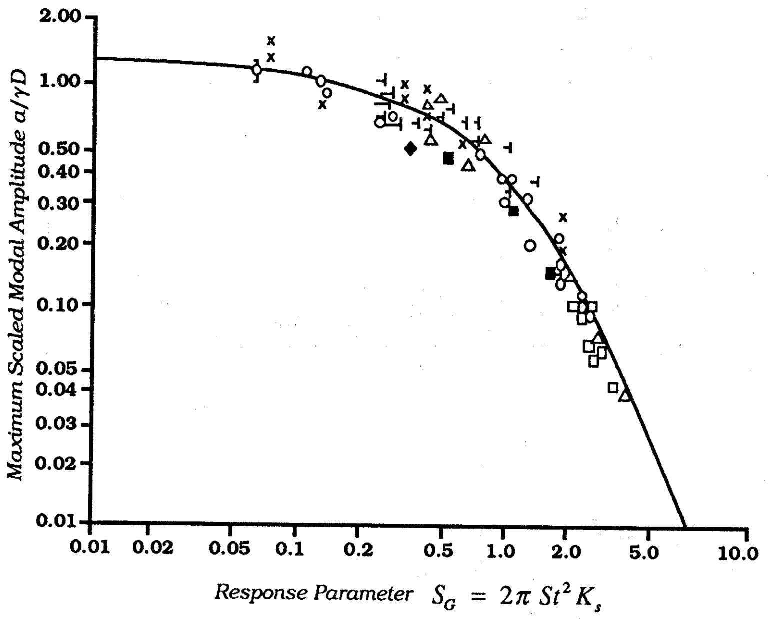

Figure 2.17
Variation of crossflow displacement with response parameter in sub-critical flow (Skop et al [18])

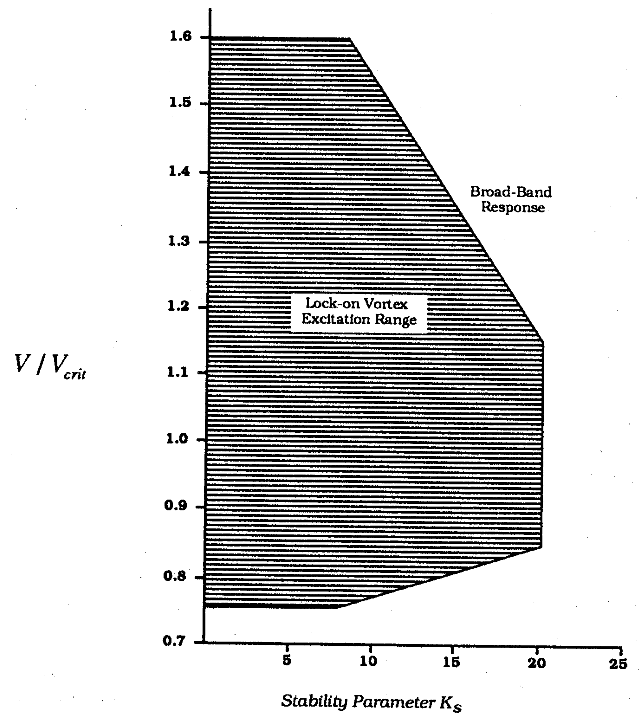

Figure 2.18
Lock-on boundary curve as a function of K$_s$

The lock-on bandwith response within the threshold range is not discussed in the DnV guidance. BS 8100 recommends a force coefficient which when corrected to allow for the velocity squared term in the excitation force, predicts a broad banded behaviour as shown in Figure 2.19. The ESDU guidance indicates that the bandwidth response is dictated by the member damping and becomes increasingly more steep as the member damping increases as shown in Figure 2.19.

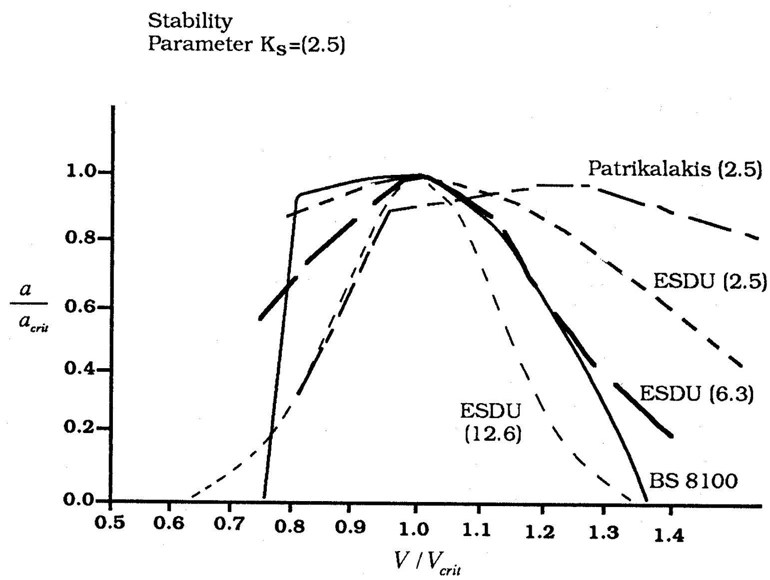

Figure 2.19
Comparison of bandwidth responses
from ESDU, BS 8100 and empirical data

Both methods tend to underpredict the member response as the velocity deviates from the critical velocity when the damping parameter is low as shown in Figure 2.19. Thus a more reasonable approach is to assume that the member response within the lock-on range is of constant amplitude as defined by the response at the critical velocity for a stability parameter of K_s of three of less. For stability parameters between three and twenty, then the response could be reduced as the velocity deviates from the critical using the ESDU design curves shown in Figure 2.3.

2.7.2 Excitation Force

Of the three methods examined, the ESDU method was the most detailed attributing the response magnitude to the following parametric effects:

i) Reynolds Number

ii) Surface Roughness

iii) Atmospheric Turbulence

iv) End Effects

v) Response Amplitude

Both DnV and ESDU quantity the effects of Reynolds number and in particular the significant drop in the magnitude of the excitation force between sub and post-critical flows. BS8100 does not recognise such an effect, but recommends a force coefficient of 0.3 which is consistent with post-critical flows but higher than the values recommended by ESDU and DnV. This upper limit value is similar to that achieved in post-critical flows by experiment as shown in Figure 2.11 and may be an upper bound value which accounts for the effects of surface roughness.

DnV doe not allow for surface roughness effects but provides a range of values for the force coefficient in any given Reynolds number which may account for roughness effects. As such it is important to use the DnV upper bound limit. ESDU do allow for roughness effects which can produce an increase in excitation force. This is only true in post-critical flows since an increase in surface roughness does not influence the excitation force in sub-critical laminar flows. However, increasing surface roughness leads to an increase in the effective Reynolds number which can cause a sub-critical flow to become post-critical. Should the degree of roughness be insufficient to create post-critical flow, then the ESDU method will tend to overpredict the excitation force.

In view of these sensitivities, any simplified procedure must provide for roughness and Reynolds number effects.

In terms of atmospheric turbulence, only ESDU allow for this effect. However, in offshore applications where the wind field is generated over the open sea, there is little variation in the turbulence intensity, ie I_u has a value of 0.11. From the ESDU data, as shown in Figure 2.6, the influence of turbulence of this level is negligible on the overall member response. However where the member is in close proximity to other large offshore structures or the shore, it may be necessary to review the effects of turbulence intensity.

The influence of end effects and spanwise coherence has been considered in the ESDU guidance and supported by empirical result as shown in Figure 2.13. The simplified ESDU methodology, Note 85039, identifies that the influence of end effect and spanwise coherence tends to disappear when the span to diameter of the member in question exceeds about 20. Sub-critical laminar flows at low span to diameter ratios tend to lead to a diminution of the excitation force, presumably due to the turbulence created around the extremities. In post-critical flows, the effect of low span to diameter ratios is to cause an increase in the excitation force as spanwise coherence increases as found by experiment. However, the experimental results as shown in Figure 2.13 indicate that the reduction of coherence with increasing span to diameter ratio reduces much less and quickly reaches a plateau when the member is vibrating than when it is stationary. The experimental data would predict that for meaningful levels of vibration, ie greater than 2%, the effect of end effects and spanwise coherence is insignificant for span to diameter rations exceeding ten. It should be noted that the natural frequency for structural members with span to diameter ratios less than ten is usually too high to be excited by wind induced vortex shedding.

A word of caution should be given about the treatment of spanwise coherence described in the detailed methodology ESDU Note 85038 from which the simplified procedure ESDU 85039 was derived. ESDU Note 83038 demonstrates a significant decrease in excitation force as expected for increasing H/D (because of the correlation effect) irrespective of the lock-on response amplitude which tends to be non-conservative at large H/D, ie greater than 20. This effect is not found to the same degree in ESDU Note 85039.

Neither DnV or BS8100 allow for the effects of the member response on the excitation force whereas both the ESDU guidance and experimental data as shown in Figure 2.12 allow for a reducing excitation force with increasing amplitude which leads to the self limiting of the vibration amplitude characteristic of vortex induced oscillations. However in practice the contributions of this effect on the response amplitude are only significant when the vibration amplitude exceeds 50% of the member diameter as show in Figure 2.17. For all intents and purposes, this amplitude is usually too onerous for design of the member unless it is very slender. Thus to ignore this effect would lead to an over conservative estimate of member responses. Thus the DnV and BS8100 guidances would tend to overpredict the responses of slender members where vibration amplitudes could safely exceed 50% of the member diameter.

One weakness of the ESDU approach is that since the excitation force is influenced by the response and vice versa, then the determination of the member response has to be resolved iteratively which means it is no amenable to a simple design procedure.

2.7.3 Responses

As noted above, neither the DnV nor BS8100 methods allow for the self limiting vibration amplitudes characteristic of vortex induced oscillations. However the experimental evidence as shown in Figures 2.15 and 2.17 demonstrate the validity of this effect. These results also demonstrate the significant role that member damping plays in determining the response of a member once the wind velocity falls within the lock-on excitation range as shown in Figure 2.18. The member damping is usually defined in terms of the stability parameter K_s as defined in Section 1.0. For aerodynamic oscillations, the major component of damping derives from the member structural damping.

From a review of the guidances and the literature there appears to be considerable confusion as to what value of structural damping should be adopted. The DnV guidance recommends a value of 0.5% for wind induced oscillations. In the case of ESDU the recommended damping levels for steel superstructures mounted on rigid foundations varies between 0.3% to 0.5%, but a value of 0.5% is recommended for steel tubes. BS810 recommends a value of structural damping of 0.24% for welded steel bracing. Clearly these guidances indicate that the level of damping can vary by as much as a factor of two which could influence the estimate of the member response by an equal amount.

The literature also reveals an equal confusion. Blevins[13] found that the structural damping for tower structures could vary between 0.15 and 1.0% and Hallam et al[16] recommends a lower threshold for fabricated steel of 0.32% but that for the spring steels (unfabricated) the damping could fall as low as 0.06 to 0.12%.

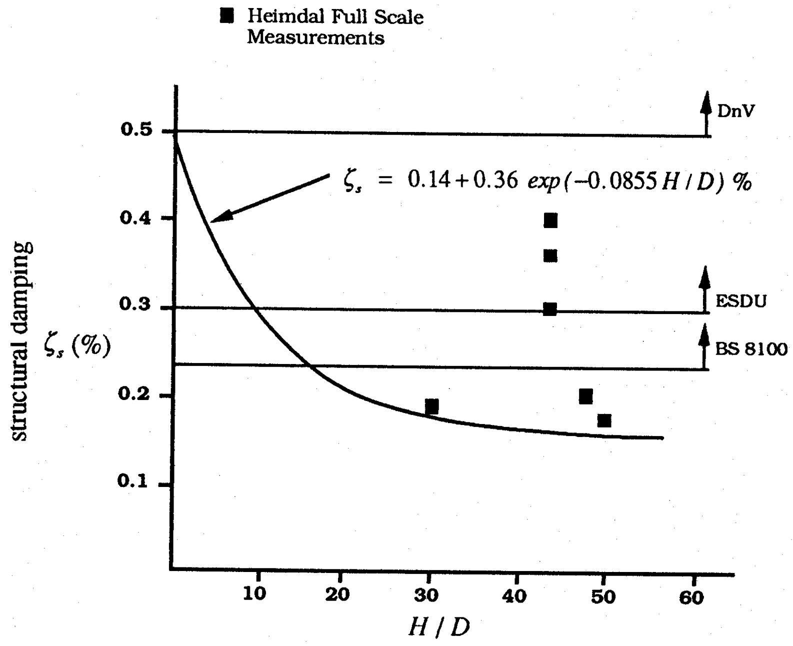

Figure 2.20
Structural damping as a function of span to diameter ratio

The Heimdal Flare boom structural damping assessment found that for members with span to diameter ratios of about 50, the structural damping value could be as low as 0.2% as shown in Table 2.5. These results also indicated that the damping increased as the span to diameter ratio increased.

Considering all this data and the range of values quoted, it appears that the structural damping of a member is not a constant but a function of the span to diameter ration as shown in Figure 2.20. This can be justified since as the nodes of an encastre member, the greatest curvatures occur causing higher strains which are dissipated in heat etc. In a very long slender member, the damping generated at the nodes becomes increasingly insignificant and the damping level approaches that associated with unfabricated steel. Thus, in any assessment of vortex shedding, the effects of span to diameter ratio on the structural damping should be taken into account. Unfortunately, little information is available in the literature to confirm this effect apart from the Heimdal measurements.

From Figure 2.20, the damping function defined in terms of the span to diameter ratio can be parameterised as:

$$\zeta_s = 0.14 + 0.36\ exp(-0.8755H/D)\%$$

Use of this latter function in combination with a Ks limit of 16 would have identified all but one of the members observed vibrating on the Heimdal platform. Increasing the stability parameter limit to 20 would have identified every observed vibrating member.

The stability parameter as dictated by the damping function above can be assessed directly by the diameter and wall thickness of thin walled steel tubular members as shown in Figure 2.21 ie:

$$K_s = 4\zeta_s\,\pi.\frac{\rho_s \pi D t}{\rho_a D^2}$$

ie $M_e = \rho_s \pi Dt$ where ζ_s is defined as shown in Figure 2.20.

Thus, for a given span, diameter and wall thickness, the stability parameter for a thin walled steel tube can be estimated from Figure 2.21.

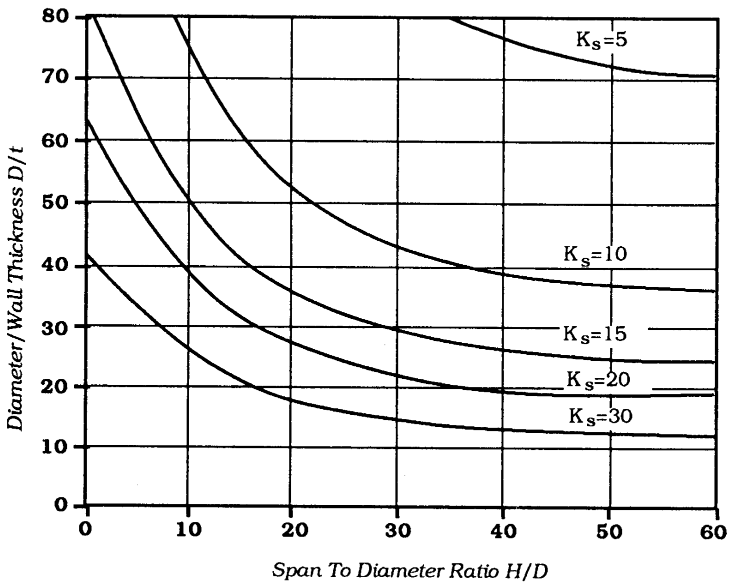

Figure 2.21
Stability parameter as a function of diameter to wall thickness and span to diameter ration for think walled steel tubes

A simplified procedure is recommended based on the work of Skop et al[18] and Sarpkaya and Issacson[10]. Skop proposes an empirical response model for predicting the amplitude of response which takes into account the self limiting amplitude effect and the stability parameter as shown in Figure 2.17 ie:

$$\frac{a}{D} = 1.29.\frac{\gamma}{[1{+}0.43(2\pi K_s St^2)]^{335}}$$

However this data is based totally on measurements in sub-critical flows and does not account for the effects of post-critical flow or surface roughness.

Sarpkaya and Isaacson[10] proposes a revised equation for the response amplitude which allows for the effect of Reynolds number and surface roughness for use in oscillatory flows. An equation for response in steady wind induced flows is presented based on the Sarpkaya and Isaacson[10] correction but adopted for steady flow conditions as given by:

$$\frac{a}{D} = \frac{3.82.Cl.\gamma}{[1{+}0.19(2\pi K_s St^2/Cl)]^{335}}$$

The effects of surface roughness and Reynolds number used in this equation are based on the data presented in ESDU Note 85038 as shown in Figure 2.22. This formulation reduces to that given by Skop et al[18] in sub-critical flows but will allow for the reduction in response characteristic of post-critical flows. This figure is derived for non turbulent flow and smooth members. The effect of turbulence and roughness reduces the transition Reynolds number. ESDU provide guidance on calculating for these effects.

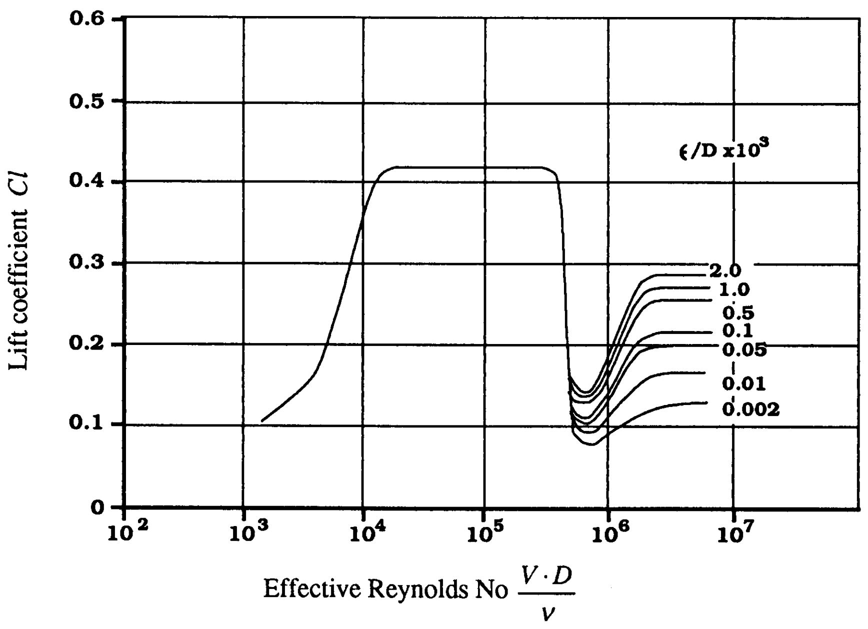

Figure 2.22
Variation of lift coefficient with surface
Roughness and Reynolds number from ESDU 85038

This simplified procedure for predicting member response accounts for the following effects:

i) Reynolds Number

ii) Surface Roughness

iii) Member Damping

iv) Influence of Response on Excitation Force

The effects of atmospheric turbulence, spanwise coherence and end effects are ignored as these are not considered significant for the typical members in offshore platform topsides such as flarebooms which are susceptible to vortex induces oscillations.

In conclusion, the following considerations should be emphasised:

i) It is best to design to avoid narrow banded lock-on response by selecting stiff structural members whose natural frequencies ensure that wind speeds are insufficient to enter the lock-on range lower limit. It is not advisable to select members of low stiffness characteristics unless they have great flexibility and resistance to fatigue, due to the potential for higher mode excitation.

ii) Marginal design of member sizes to just avoid the critical velocity range should be avoided due to the uncertainties in predicting the member natural frequency.

iii) The uncertainties in predicting member response is still significant.

To design a structure for the worst combination of all possible assumptions would be exceedingly onerous. However, to design a structure where a considerable number of the members are marginal using “median” assumptions would result in a high risk of local structural damage.

3. SIMPLIFIED DESIGN PROCEDURE

The most rational design approach to preventing structural problems due to vortex induced oscillations is to identify member properties which can be demonstrated to lead to acceptable stresses in terms of both fatigue and ultimate strength.

It should be noted that the number of cycles associated with typical vortex induces oscillations will tend to exceed the number associated with the stress range cut-off of a typical S-N curve unless the wind conditions which cause vortex induced oscillations occur infrequently, eg less than 10% of the time. Checks should therefore be performed that the occurrence of wind conditions which can excite the structure are sufficiently infrequent to prevent unacceptable fatigue damage.

The member should be sized in order to ensure that the vortex induced stresses are acceptable by careful selection of the member geometric properties both to achieve adequate structural damping and a high enough natural frequency so that it is excited into lock vibrations infrequently or preferably not at all.

The simplified procedure is shown as a flow chart in Figure 3.1.

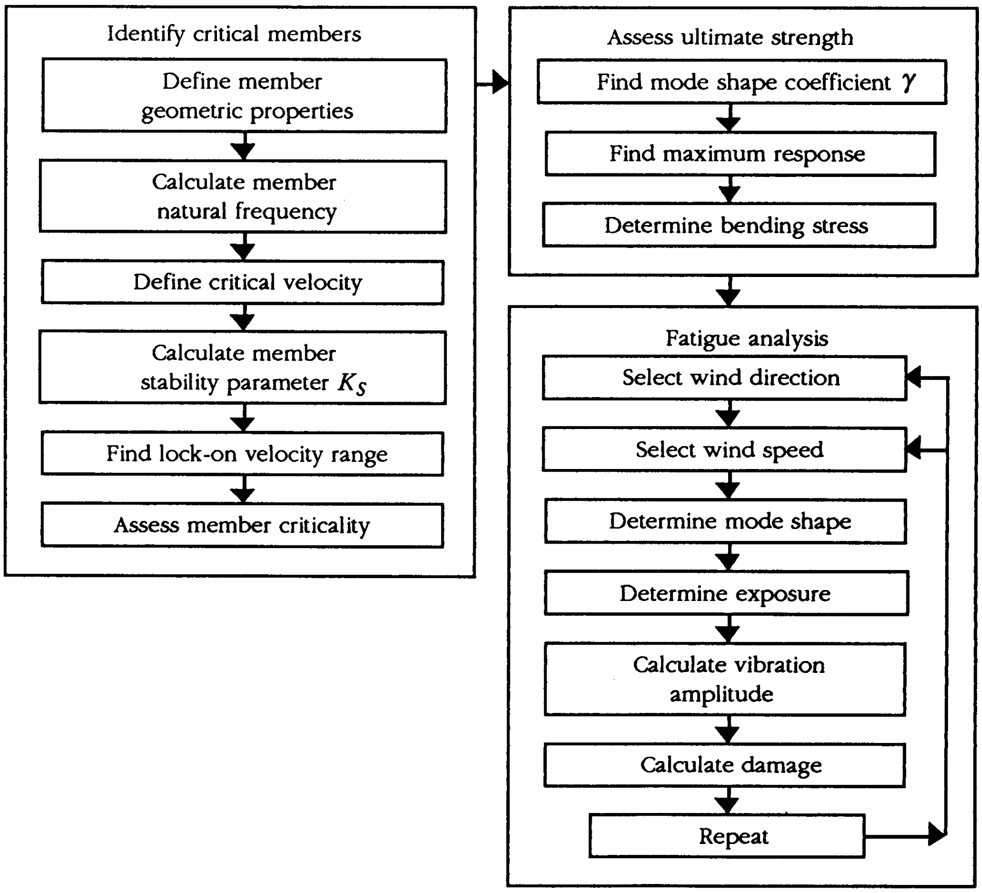

Figure 3.1
Simplified analysis procedure

3.1 IDENTIFICATION OF CRITICAL MEMBERS

A simple screening method is recommended based on the member or sub-structure geometric properties which can rapidly identify critical elements within a structure and consisting of the following steps:

1. Define Member Geometric Properties

Assemble geometric properties of the member to be screened *(H,I,D,E,M(z)...)*.

2. Calculate Member Natural Frequency

Determine the natural frequency *Ns* for each transverse mode considered critical for the member or sub-substructure, as based on the member mass and stiffness properties. Properties of simple beams not subject to significant axial tension or compression are given in Table 3.1. It is recommended that the sensitivity of the vortex induced stressed to the assumed member support constraints be reviewed.

The effects of end fixity and preload (tension and compression) should be considered in the evaluation of the member or sub-structure natural frequency.

Figure 3.1
Sample values of parameters for uniform beams

Mode Shape	Natural frequency factor 1st Modes only $A1 = 2\pi N_s \frac{H^2}{\sqrt{EI/M_e}}$	Mode shape Co-eff (Van der Pol) γ	Bend moment factor $F_{BM} = \frac{BM}{E1a/H^2}$
Simply supported	9.87	1.155	9.87
Encastre-Pinned	15.42	1.161	20.40
Encastre-Encastre	22.37	1.167	28.20
Encastre-Free (Cantilever)	3.52	1.305	3.52

3. Define Critical Velocity

Determine the critical velocity based on the Strouhal number as given in Figure 3.2, ie:

$$V_{crit} = \frac{D.N_s}{St}$$

Note for vibrating cylinders, the lower bound Strouhal number should be adopted in the post-critical flow regime.

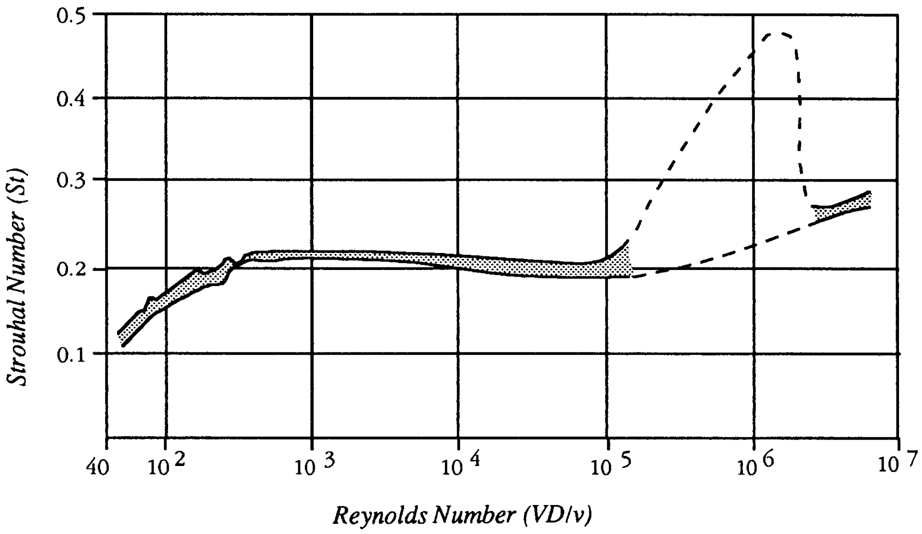

Figure 3.2
The Strouhal-Reynolds number relationship
for circular cylinders

4. Calculate Member Stability Parameter

Determine the stability parameter using the formulae:

$$K_s = \frac{4\pi.\zeta_s.M_e}{\rho_a.D^2}$$

Where the structural damping ζ_s can be determined from the span to diameter ration *H/D* as shown in Figure 3.3.

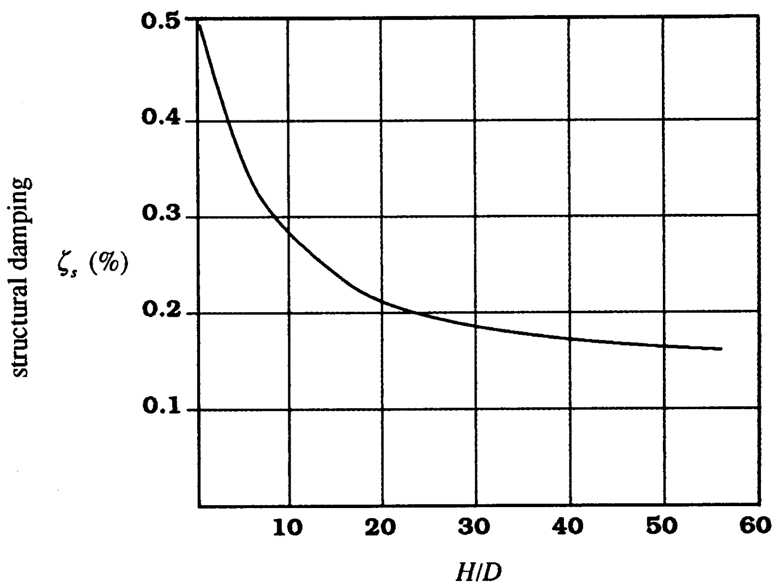

$$\zeta_s = 0.14 + 0.36\,exp(-0.0855H/D)\ \%$$

Figure 3.3
Structural damping as a function
of span to diameter ratio

5. Define Lock-on Velocity Range

From the critical velocity and the stability parameter, define the onset velocity for lock-on response based on Figure 3.4. Note that this is the velocity which is normal to the member or sub-structure at mid span. The wind velocity should be determined from the resolved member-velocity.

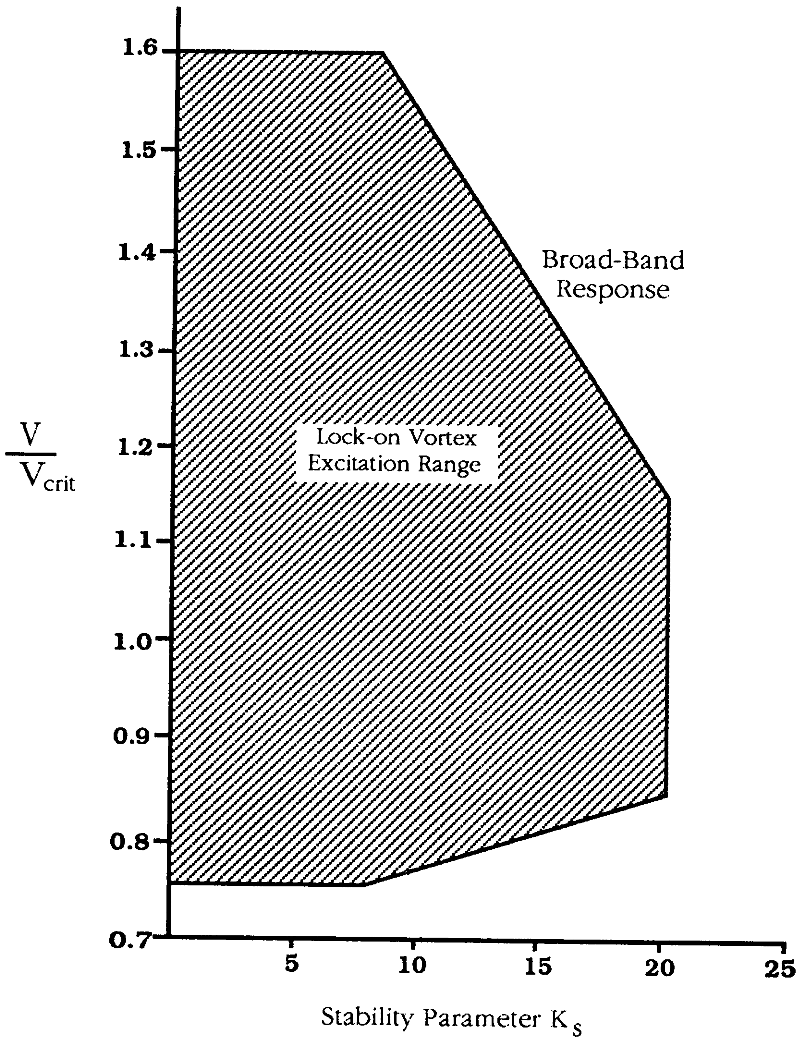

Figure 3.4
Lock-on boundary curve

6. Critical Member Assessment

Determine whether this wind condition will occur in the lifetime of the structure. Note this depends on the accuracy of the natural frequency estimate. If the wind condition does not occur, then the member or sub-structure can be assumed as insensitive to vortex induced oscillations.

If the wind condition does arise, then both the ultimate strength capacity and fatigue life of the member should be assessed as defined in Sections 3.2 and 3.3.

If the fatigue life due to vortex induced oscillations is found to be unacceptable or the members' ultimate strength capacity is found to be inadequate, then the member section properties should be revised. Note when assessing fatigue damage that some consideration should be given to other dynamic loading effects such as wind gust excitation or buffeting of the structure.

3.2 ULTIMATE STRENGTH CAPACITY

Once a member has been identified as critical, then the ultimate strength capacity should be checked using the worst environmental wind condition corresponding to V_{crit} for the highest mode likely to be excited. The following procedure is recommended:

1. Determine Mode Shape Coefficient

Identify the highest mode shape excitable within the design range of wind speeds.

Assess the γ parameter for the member as based on its expected mode shape, ie:

$$\gamma = \sqrt{\frac{\int_O^H u(z)^2 dz}{\int_O^H u(z)^4 dz}}$$

Values for uniform beams with a number of support conditions are given in Table 3.1.

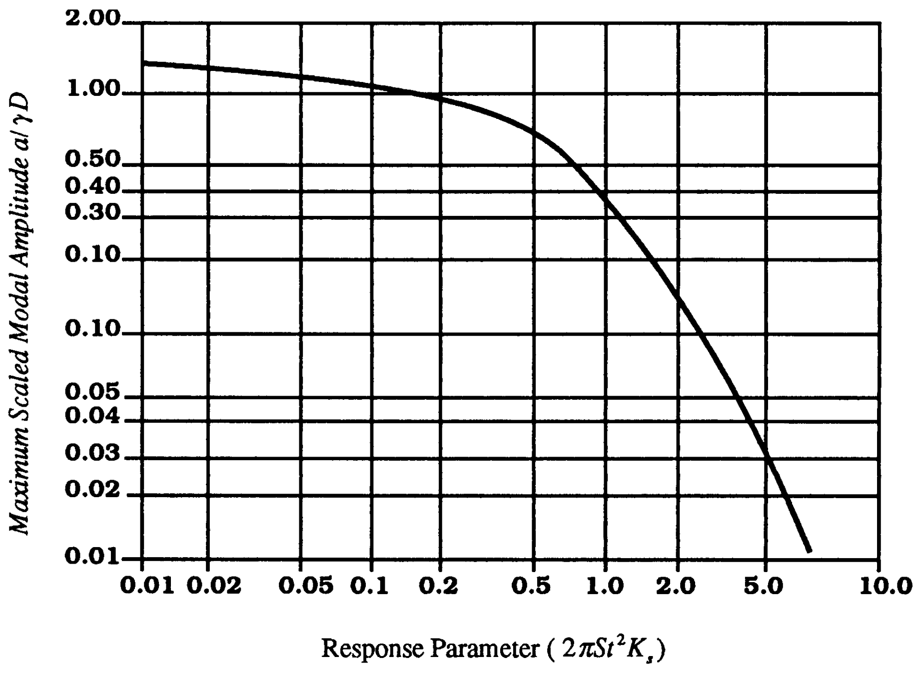

Figure 3.5
Variations of scaled modal amplitude versus response parameter

2. Determine Maximum Response Amplitude

Determine the maximum response amplitude for the member of structural component from the following narrow banded response formulation (Figure 3.5):

Where:

$$\frac{a}{D} = \frac{3.82.Cl.\gamma}{[1+0.19(2\pi K_s St^2 Cl]^{335}}$$

γ	is the Van der Pol mode coefficient defined above.
Cl	is the lateral (lift) force coefficient based on the Reynolds number and surface roughness as shown in Figure 3.6. Note that transition is based on non turbulent flow and smooth cylinders.
St	is the Strouhal number as defined above.
K_s	is the stability parameter as defined in Section 3.1.

Note that the guidance for choosing the value of the roughness parameter $\in$ and calculating the effective Reynolds number is given in ESDU 85038.

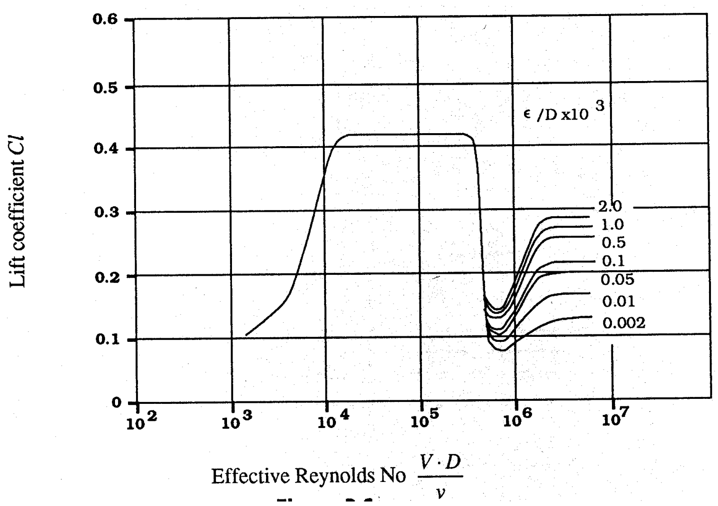

Figure 3.6
Variation of lift coefficient with surface roughness and Reynolds number from ESDU 85038

If the resulting amplitude of vibration is less than 2% of member diameter, a broad band calculation would be more appropriate. However, the narrow band calculation will give a quick conservative estimate of maximum stress.

3. Determine Corresponding Bending Stress

Determine the maximum bending stress in the member of sub-structure by applying a deflection profile based on the maximum amplitude and the mode shape.

4. Check Member Strength Adequacy

Confirm that the maximum stress does not exceed the allowable using appropriate material and load factors and including all other load contributions from dead and live loads corresponding to this environmental condition.

If the strength is estimated to be inadequate for a member subject to broad band excitation, a more detailed check should be carried out according to ESDU 85038 or ESDU 85039.

3.3 FATIGUE ANALYSIS

The most likely mechanism for structural failure from vortex induced excitation is fatigue. The following procedure is proposed to assess the fatigue life of structural members or sub-structures subject to vortex induced excitation.

1. Define Wind Velocity Ranges

Identify the wind velocities normal to the member which fall within the lock-on ranges for each mode that can be excited as identified in Section 3.1. Assume that only one mode can occur simultaneously. If more than one mode co-exists for a given wind velocity, the lock-on limit boundaries should be defined by the mode whose reduced velocity is closest to the critical reduced velocity.

For each quadrant of the wind field, determine the wind conditions which produce normal velocities within the lock-on range for each mode of the member or sub-structure. It is recommended that the cumulative probability distribution for a one hour mean wind speed is adopted.

2. Define Stress Ranges

Determine the maximum stress range (ie twice the stress amplitude) for the critical velocity from the response amplitude for each mode as identified in Section 3.2.

Subdivide the lock-on velocity range and calculate the stress ranges for each member based on the stress range at the critical velocity and the response envelope as defined by the stability parameter for narrow banded processes shown in Figure 3.7.

For members with partial or total end fixity, calculate the stress ranges at the structural connections. Calculate the stress concentration factors to be applied to the stress range data corresponding to the joint construction and loading pattern, select the corresponding fatigue curve, and determine the number of cycles to failure.

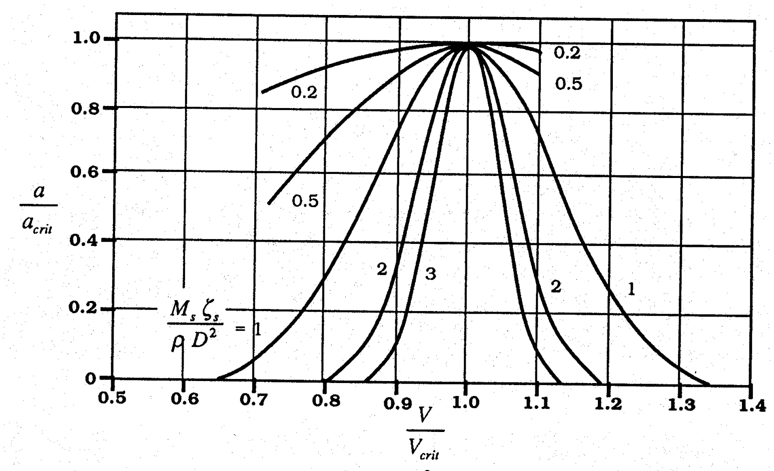

$M_s \zeta / (\rho_a D^2) = K_s / 4\pi$

Figure 3.7
Variation of narrow banded response amplitude
V/V_{crit} as a function of stability parameter K_s

If the member response amplitude is less than 2% of the member diameter, and K_s is greater than 20, then the more conservative broad band response bandwidth should be used as shown in Figure 3.8 (based on atmospheric turbulence I_u = 0.20). However if the fatigue lift is found to be unacceptable, the damage can be revised using the less conservative board band critical response, as discussed in Section 2.3.3.

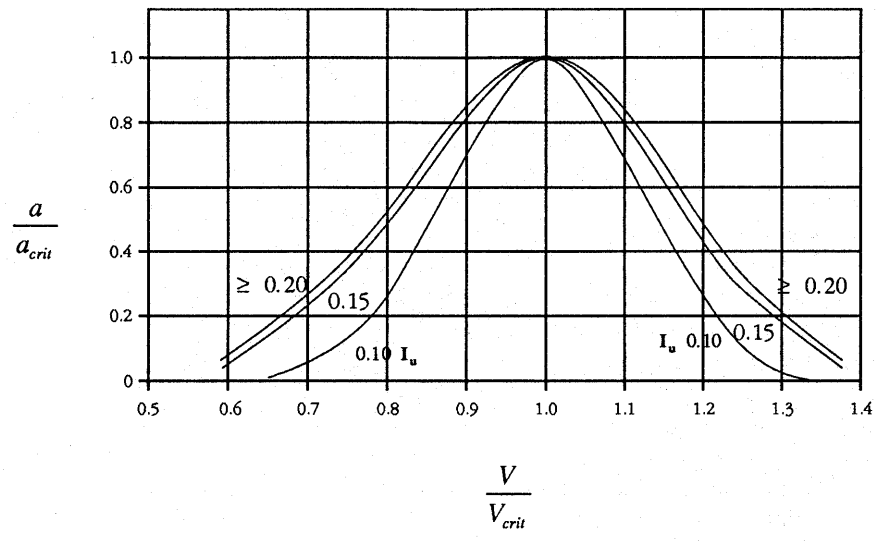

Figure 3.8
Variation of broad banded response amplitude with
V/V_{crit} as a function of turbulence intensity/$_u$

3. Define Probability of Occurrence

Determine the cumulative probability of occurrence of wind speeds which fall within each sub-element of the lock-on range and identify the number of load cycles per annum based on the member modal period. It is recommended that the fatigue damage assessment should be for at least the expected lifetime of the structure. Occurrences of wind conditions can be determined from BS8100 in the absence of more specific field data.

4. Determine Fatigue Damage

Determine the Cumulative fatigue damage per annum for all directions, lock-on ranges and wind speeds within the lock-on range using Miners Rule and the appropriate S-N curve ie:

$$\text{fatigue damage per annum} = \underbrace{\sum_{i}}_{\text{wind direction}} \underbrace{\sum_{j}}_{\text{mode shape}} \underbrace{\sum_{k}}_{\text{wind speed}} \frac{n(i,j,k)}{N_f(i,j,k)}$$

where

n(i,j,k) is the number of vibration cycles for a sub-element of the wind speed lock-on region for a given mode shape and wind direction.

$N_f(i,j,k)$ is the number of cycles to failure for the stress range corresponding to the sub-element parameters.

5. Assess Fatigue Criticality

Add the fatigue damage arising from all other sources and determine the fatigue life of the structure.

Note that for simple procedure it has been assumed that the maximum stressed due to the different modes all occur at the same place (normally the ends), however this may not be the case, and account could be taken if appropriate of reductions in the fatigue damage due to the damage from the different modes occurring predominantly in different places.

3.4 METHODS OF SUPPRESSING VORTEX EXCITATION

When the response to vortex shedding produces unacceptable stresses, considerations must be given to reducing the amplitude of response. Suppression of vortex induced vibration can be achieved using mechanical or fluid dynamic means in the following ways:

- **Changes in member properties and structural detailing**
  Increases in the natural frequency, stiffness or damping, either singly or in combination, will generally reduce the oscillation amplitude. by simply increasing the diameter of a member, a typical design approach, it may be possible to achieve a critical velocity which is higher than the maximum design wind speed. Note, however, that this particular approach demands caution due to the inherent uncertainty in estimating natural frequency.

  In marginal cases, as an alternative to resizing the member, a weight efficient solution may sometimes be achieved by introducing thickened stubs on the ends of hot braces (cones and pup pieces may also be added). This will reduce locally the hot spot stress and may allow the use of improved fatigue performance welds.

  Remedial measures can consist of introducing post tensioned wires at midspan in the plane of vibration or alternatively introducing a midspan support member.

- **Aerodynamic spoilers**

  These are intended to reduce the amplitude of response of disrupting the fluid processes involved in vortex formation. The interaction affects the shedding mechanism primarily by interfering with the wake and reducing spanwise coherence.

  Numerous suppression devices have been proposed, including a helical strakes and windings, porous and slatted shrouds, and splitter plate devices. These are reviewed by Zdrakovich [19] and Sarpkaya and Isaacson [10]. Guidance on the design of such spoilers is given in ESDU 85038[2].

  Note that the fitting of spoilers increases the in-line drag coefficient on cylinders, particularly in the post-critical Reynolds number regime. Turbulen buffeting loads are correspondingly increased and may become critical.

Of the mechanical and fluid dynamic solutions offered above, the former would generally be used at the design stage whereas the latter would be considered if in-situ problems were encountered.

4. WORKED EXAMPLES

Two worked examples are presented, both of which are identified as critical. The examples chosen are based on prototype structural members as identified in Figure 4.1. Member 1 was observed vibrating in wind as shown on Table 2.4, however the second member was not observed to vibrate.

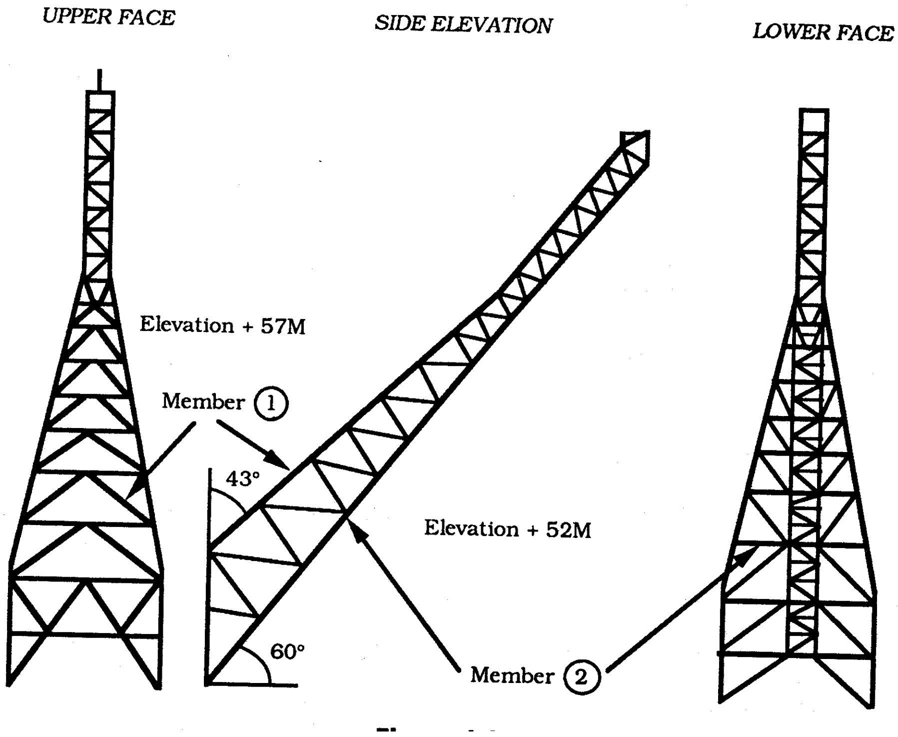

Figure 4.1
Location of worked examples in prototype structure

4.1 IDENTIFICATION OF CRITICAL MEMBERS

The two members selected are subject to the simplified procedure (Table 4.1). Both members are identified as critical and calculations were pursued. The geometry and location of these members is shown in Figure 4.1.

4.2 ULTIMATE STRENGTH CAPACITY

The critical member assessment identified that Member 1 was highly susceptible to narrow banded vortex induced excitations. In the case of Member 2, it was identified as subject to broad banded excitation infrequently. An ultimate strength capacity analysis is shown to identify each member's capacity to tolerate the maximum possible vortex induced vibrations. The calculation (Table 4.2) is based on the first mode of vibration only.

The load factors demonstrate that the responses will produce levels of stress when excited that are acceptable. However, these should be superimposed on the bending and axial stresses due to other load effects. It should be noted that the significant wind speed for excitation of the second mode of the first member will fall within the wind velocity range for the structure and if excited would lead to unacceptable stresses for that member. In the case of the second member, the critical wind velocity for the second mode was well above the design wind velocities.

4.3 FATIGUE ANALYSIS

Fatigue analyses are presented for each member identified as critical. For the sake of simplicity, the effects of wind directionality have not been taken into account, and the analysis is thus conservative.

Table 4.3 confirms that whereas member 2 was acceptable, member 1 is unacceptable and should be re-sized.

Calculation notes on Table 4.3

Minimum and maximum velocity ratings are V_{on}/V_{char} and V_{up}/V_{char}. Values in columns 2 and 3 are the bounds of each sector (10 equal sectors have been used).

The maximum stress range, σ, is here assumed to be given in units of Newtons/mm₂.

Wind probability of occurrence data based on BS8100 and a characteristic wind speed of 25m/s has been used in the analysis.

Table 4.1
Identification of critical members
(uniform tubular)

Item No	Item	Variable	Symbol	Member No 1	Member No 2	Units
1	Define global constants	Density of air	ρ_a	1.222	1.222	kg/m^3
		Viscosity	v	1.5X10^{-5}	1.5X10^{-5}	m^2/s
		Strouhal number	St	0.2	0.2	
		Youngs modulus	E	210	210	kN/mm^2
		Density of steel	ρ_s	7.85	7.85	Te/m^3
		Allowable stress	σ_A-0.75 x *yield*	255	255	N/mm^2
2	Define members properties	Length	H	15.2	8.3	m
		Diameter	D	273	273	mm
		Wall thickness	t	7.8	18.3	mm
	Note: fixed-pinned (able 3.1)	Frequency coefficient	A_1	15.42	15.42	
		Bend mom coefficient	F_{BM}	20.44	20.44	
		Van der Pol	γ	1161	1.161	
3	Calculate natural frequency	Mass per unit length	$M_e=\rho_s\pi t(D-t)$	51.0	115.0	kg/m
		Moment of inertia	$I= \frac{\pi}{4}.[(\frac{D}{2})^4-(\frac{D}{2}-t)^4]$	57.10^{-6}	119x10^{-6}	m^4
		Natural frequency	$N_{s+\frac{A_1}{2\pi H^2}\cdot\sqrt{\frac{EI}{Me}}}$	5.15	16.6	Hz
4	Define critical velocity		$V_{crit}=\frac{D.N_s}{St}$	7.03	22.7	m/s
5	Calculate member stability parameter	Structural damping	ζ_s+0.14 +0.36*exp*(-0.0855*H/D*)	.143	.167	%
		Stability parameter	$K_s=4\pi Me.\frac{\zeta_s}{\rho_a D^2}$	10.07	26.5	
6	Find lock-on velocity range .. from Figure 3.4	Narrow(N) or broad(B)	band Ks<20?	N	B	
			V_{on}	5.40	17.03	m/s
		Onset velocity	V_{up}	10.71	36.33	m/s

Note: lock-on range wider for broad turbulence (I_u=0.1 assumed)

Both member 1 and member 2 may be subject to vortex induced excitation although member 2 is broad band due to the high value of K_s.

Table 4.2
Assess ultimate strength

Item No	Item	Variable	Symbol	Member No 1	Member No 2	Units
7.	Find mode shape coefficient (Table 3.1)		γ	1.161	1.161	
8.	Find maximum response	Reynolds number	$R_e = \frac{V_{crit} D}{\upsilon}$	1.3×10^5	4.13×10^5	
		Response parameter	$S_G = 2\pi . St^2 . K_s \, Cl$	2.53	6.65	
	Figures 3.5 and 3.6	Lift coefficient		0.42	0.29	
		Maximum amplitude	$a = \frac{3.82 \gamma Cl D}{(1+0.19 \frac{S_G}{Cl})^{335}}$	39.4	1.2	mm
9.	Find bending stress	Bending moment	$BM = a.F_{BM} . \frac{EI}{H^2}$	41.9	8.9	kNm
		Bending stress	$\sigma = \frac{D}{2} . \frac{BM}{I}$	100.	10.	N/mm^2
		.. of allowable	σ / σ_A	0.39	0.04	

Both members pass the strength check, as based on narrow banded responses.

Table 4.3
Fatigue analysis

Characteristic wind speed from BS 8100 V_{char}=25.00 m/s

Joint SCF=2.500

Member angle to wind=0 degrees

Member 1

	Ratio to characteristic velocity					X-Fatigue curve		BS8100	
Fatigue cells	Onset velocity ratio	Upper velocity ratio	Mean velocity ratio	Vmean/ Vcrit	Stress range N/mm^2	cycles to failure	hours to failure	hours exposure	Fatigue damage per annum
1	0.216	0.237	0.23	0.81	233	73665	4	382.	96
2	0.237	0.258	0.25	0.88	375	10368	.6	382.	684
3	0.258	0.280	0.27	0.96	481	3742	.2	382.	1896
4	0.280	0.301	0.29	1.03	490	3462	.2	382.	2049
5	0.301	0.322	0.31	1.11	355	13054	.7	382.	543
6	0.322	0.343	0.33	1.18	184	192207	10	382.	637
7	0.343	0.365	0.35	1.26	68	11505075	620	1000.	1.6
8	0.365	0.386	0.38	1.33	18	2.00E+08	10780	392.	0.036
9	0.386	0.407	0.40	1.41	3	2.00E+08	10780	284.	0.026
10	0.407	0.428	0.42	1.48	0	2.00E+08	10780	205	0.019
This member will fail the fatigue check							Total	4175	5308

Member 2

Broad band calculation, $I_u=0.1$

Fatigue cells	Onset velocity ratio	Upper velocity ratio	Mean velocity ratio	Vmean/ Vcrit	Stress range N/mm^2	cycles to failure	hours to failure	hours exposure	Fatigue damage per annum
1	0.681	0.758	0.72	0.79	14	2.00E+08	3340	7.97	0.002
2	0.758	0.836	0.80	0.88	32	2.00E+08	3340	2.46	0.001
3	0.836	0.913	0.87	0.96	49	4.50E+07	753	0.76	0.001
4	0.913	0.990	0.95	1.05	47	5.00E+07	835	0.24	0.00
5	0.990	1.067	1.03	1.13	30	2.00E+08	3340	0.07	0.000
6	1.067	1.144	1.11	1.22	12	2.00E+08	3340	0.02	0.000
7	1.144	1.222	1.18	1.30	3.3	2.00E+08	3340	0.01	0.000
8	1.222	1.299	1.26	1.39	0.6	2.00E+08	3340	0.00	0.000
9	1.299	1.376	1.34	1.47	0.07	2.00E+08	3340	0.00	0.000
10	1.376	1.453	1.41	1.56	0.0	2.00E+08	3340	0.00	0.000
							Total	11.54	0.004

This member passes the fatigue check for vortex shedding effects (life=224 years)

5. REFERENCES

1) Rules for the Design, construction and Inspection of Offshore Structures, 1977,. Appendix B Loads, reprinted with corrections 1982, Det norske Veritas

2) Engineering Sciences Data Unit (ESDU) Data Item Numbers: (Circular Cylindrical Structures, Dynamic Response to Vortex Shedding), 85038 pt 1, Calculation Procedures and Derivation, 85039 pt 2, Simplified Calculation Procedures, 85040 pt 3, Computer programs

3) British Standard Lattice Towers and Masts, Part 1, Code of Practice for Loading, BS8100, Part 1, 1986

4) Woo, HCG, Peterka, JA and Cermak, JE, “Experiments on Vortex Shedding form Stationary and Oscillating Cables in a Linear Shear Flow”, Final Report, Contract N68305-78-C-005, Naval Civil Eng Laboratory, Colorado State University, July 1981.

5) Peltzer, RD, “Vortex Shedding from a Vibrating Cable with Attached Spherical Bodies in a Linear Shear Flow”, Naval Research Laboratory Memorandum Report 4940, October 1982.

6) Standsby PK, “The locking-on of Vortex Shedding due to Cross Flow Vibration of Circular Cylinders in Uniform and Shear Flows”, Journal of Fluid Mechanics, 74, 1976, pp 641-667.

7) Koopman, GH, “The Vortex Wakes of Vibrating Cylinders at Low Reynolds Numbers”, Journal of Fluid Mechanics, 28, 1967, pp 501-512.

8) Patrikalakis, N M, and Chryssostomidis, C, “Theoretical and Experimental Prediction of the Response of Marine Riser Model in a Uniform Stream”, Report MITSG 83-15, August 1983, Massachusetts Institute of Technology, Cambridge, USA.

9) Feng, G C, “The Measurement of Vortex Induced Effects in Flow Past Stationary and Oscillating Circulator and D-Section Cylinders”, MA Sc. Thesis, University of British Columbia, 1968.

10) Sarpkaya, T, and Isaacson, M, “Mechanics of Wave Forces on Offshore Structures”, Chapter 8, 1981, Van Nostrand Reinhold Company, New York.

11) Vickery, B J, and Watkins, R D, “Flow Induced Vibration of Cylindrical Structures”, Proceedings of the First Australian Conference, University of Western Australia, 1962.

12) Hartlen, R T, Baines W D and Currie I G, “Vortex-Excited Oscillations of a Circular Cylinder” Report UTME-TP 6809, 1969, University of Toronto.

13) Blevins, R D, “Flow Induced Vibration”, 1977, Van Nostrand Reinhold Company, New York.

14) Toebes, G H, “The Unsteady Flow and Wake Near an Oscillating Cylinder”, Journal of Basic Engineering, 91, pp 493, 1969.

15) Vandiver, J K, “The prediction of Locking Vibration on Flexible Cylinders in a Sheared Flow”, OTC 5006, Offshore Technology Conferences, Houston, 1985.

16) Hallam, M G, Heaf, N J, and Wootton, L R, “Dynamics of Marine Structures”, report UR8, 1978, CIRIA Underwater Engineering Group, London.

17) Doucet, Y J, and Nordhus, A, “Vibration Monitoring of a Flare Boom”, OTC 5523, Offshore Technology Conference, Houston, 1987.

18) Skop, R A, Griffin, O M and Ramberg, S E, “Strumming Predictions for the SEACON11 Experimental Mooring”, OTC 2884, Offshore Technology Conference, Houston, 1977.

19) Zdravkovich, M M, “Review and Classification of Various Aerodynamic and Hydrodynamic Means for Suppressing Vortex Shedding”, Journal of Wind Engineering and Industrial Aerodynamics, 7, 1981, pp 145-189.

20)